Project Number: CHE-WMC-1988

Protein Electrophoresis Across Phase Boundaries in a U-Tube

A Major Qualifying Project Report

Submitted to the Faculty

of the

WORCESTER POLYTECHNIC INSTITUTE

in partial fulfillment of the requirements for the

Degree of Bachelor of Science

in Chemical Engineering

by

Andrew Laflash

Anna Maziarz

Brian Mercer

Erik Newman

Date: April 28, 2011

Approved:

Prof. William M. Clark, Major Advisor

Key Words:
Two-Phase Electrophoresis, Multi-physics Modeling, Dextran, Polyethylene glycol, Hemoglobin

Abstract

The overall purpose of this Major Qualifying Project was to investigate the feasibility of using an electrical current to drive protein separation in a two phase electrophoretic system. The idea for the project originated from the discrepancy between two papers. One by Levine-Bier stated that little or no protein would be able to cross the interface from the preferred phase to the non-preferred phase regardless of current or time. Clark-Marando stated that with an appropriate electrical current and given enough time the protein would cross from preferred to non-preferred. The potential importance of this research was the possible implications for separating desired proteins from undesired waste in industry.

The project started as a replication of the conditions that Levine-Bier used as their primary case in their paper, with minor modifications. As research continued the conditions were modified to produce more appreciable results without modifying the core principles of the experiment. Solutions of various concentrations of protein, dextran, and PEG at pH11 and pH9, also used as the primary case for Levine-Bier, were tested in a short U-Tube.

The numerical model was generated in COMSOL 3.5 as a 2-D representation of a U-Tube, assuming equilibrium at the phase interface, using Electro-kinetic Flow and Conductive Media DC equations. The resulting images exhibited a successful migration of the protein across the phase interface at various partition coefficients. As Levine-Bier conclusions stated, the model also showed the protein accumulation occurs at the interface, especially at low partition coefficients, although when the run was extended and if the electric field strength was increased, the protein moved across the phase and reached the top of the non-preferred phase.

The experiments consisted of eight runs using various U-Tubes and solutions to determine the ability of the protein to move from the preferred to the non-preferred phase. The experimental results exhibited that pH 9 solutions had a limited protein migration towards the cathode, where pH 11 solution had protein migration towards the anode. A temporary holdup of protein did occur on the interfaces. It was concluded to be a result of a local equilibrium. However, it was seen that the protein continued to move across the interface contrary to what Levine-Bier stated in their paper.

The conclusions from the experimental data allowed the following recommendations to be made. The U-Tube should be made out of a tube with a larger internal diameter, the length between the electrodes should be decreased, and a power supply that is capable of supplying more than 3000 V. It is also recommended that a controlled environment that holds the temperature between 3 and 4°C be developed to run the experiments in, the experimental setup should involve a way of circulating buffer to avoid buffer ion depletion.

It is also recommended that the experiments be run with solutions at pHs other than the ones tested in this paper, as well as with higher partition coefficients.

Table of Contents

Table of Tables

Table of Figures

Introduction

In the separation industry many different tactics are employed to isolate particular compounds or substances from a mixture. Electrophoresis is one such technique of separation. This technique involves the use of an electrically charged aqueous system containing a substance that is attracted or repulsed by the electric field. This causes the substance to migrate towards, or away from, the charge emitters, or probes in the cause of our experiments, effectively separating the substance from the surrounding liquid. Electrophoresis is generally preformed in a single phase solution which allows the particles to move with relative ease within the solution once an electrical charge is applied. However, in our experiments we were primarily studying the effects of electrophoresis across a phase boundary in a two-phase liquid mixture. The main goal was to determine in an electric field can be utilized to cause hemoglobin to transfer across the phase barrier of a two-phase system from the preferred phase to the non-preferred phase.

For the basis of our experiments we primarily used two different papers on the subject of two-phase electrophoretic systems. The first was written by Michael A. Marando and William M. Clark which discussed their experiments in utilizing two-phase electrophoretic systems to separate hemoglobin. (Clark & Marando, 1993) The two-phase solution was composed of polyethylene glycol with molecular weight of 500,000, dextran with an average 8000 molecular weight, trizma base, deionized water further purified with Millipore Milli-Q filtration, and hemoglobin. The apparatus that they used was cylindrical in shape and was partitioned into 3 chambers separated by Millipore PLGC 10,000 NMWL membranes, as shown in Fig. 1, which allowed electrical current to pass through but not the solutions. The top and bottom chambers each held an electrode, formed from platinum wires connected to a power supply, in solutions of the trizma buffer containing neither the protein nor the phase forming polymers. The middle chamber is where the solution containing the hemoglobin was inserted after it has settled into two-phases. The apparatus worked by having the electrodes produce a determined current which electrically charged the system causing the hemoglobin to transfer from the preferred phase to the non-preferred phase. From the experiments that were performed by Marando and Clark using buffer solutions with varying pH values, various charges, and concentrations of the PEG and dextran solution they concluded that a two-phase system is able to transfer the protein across the phase barrier with little to no resistance observed around the phase barrier.

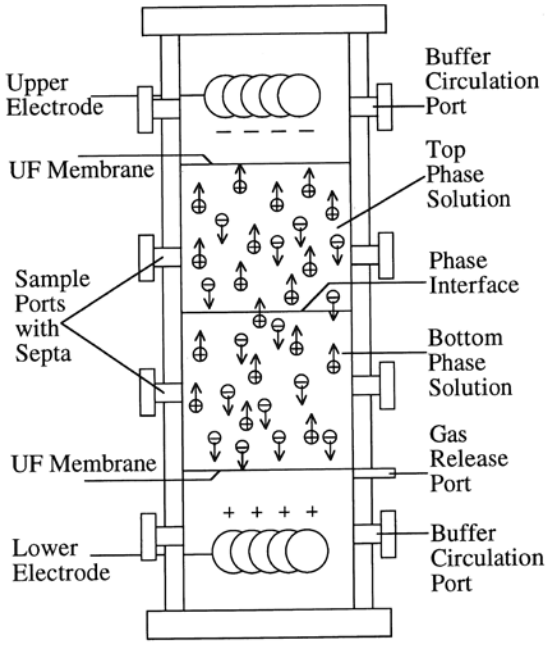

Figure 1: Marando & Clark's Two-Phase Electrophoresis Apparatus

The other paper that we looked at was written by Mark L. Levine and Milan Bier and discussed how protein transfer in the two-phase aqueous solution experiments they performed are impeded by the phase barrier. (Levine & Bier, 1990) They used the same materials as the Marando & Clark paper but with a vastly different apparatus for testing. Levine and Bier decided to use a u-tube apparatus, as shown in Fig. 2 below, that would work the same as the cylindrical apparatus in that electrodes, now located in the reservoirs of each leg of the apparatus, would cause a current to charge the system and make the protein, hemoglobin obtained from Levine's blood, move from the preferred phase into the non-preferred phase. So their experiments worked in same way as the ones that Marando and Clark preformed but Levine and Bier observed some particularly different results. Levine and Bier found experimentally that when the protein would transfer across the phase barrier when it was moving from the non-preferred phase to the preferred one but not in the opposite way despite the electrical current and despite holding the charge for two hour durations in some of the experiments. These results are in direct objection to the ones that Marando and Clark discussed in their paper.

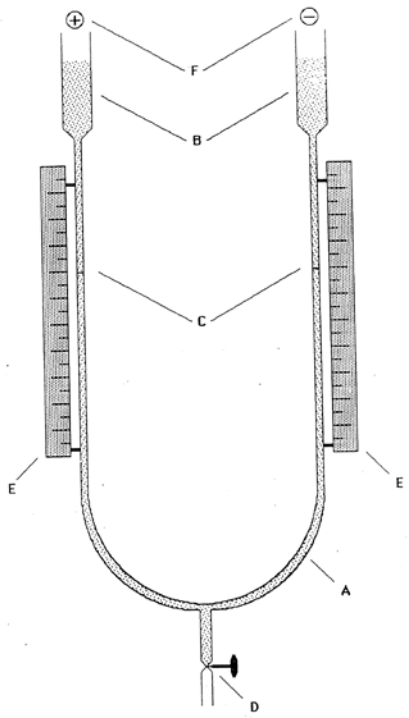

Figure 2: Levine and Bier's U-tube Apparatus

From these two papers we decided we would attempt to find out which paper was correct in their conclusions. So we decided to model our experiments after the ones that Levine and Bier conducted as their apparatus was easier to work with and construct given the materials at our disposal. Our materials for our experiments also matched that of both papers although we decided to use bovine hemoglobin as Marando and Clark used instead of separating it from a sample of human blood. With the information given in each of these papers and with having access to the correct materials to replicate the Levine and Bier experiments we proceeded to design and conduct our own experiments in order to determine whether or not protein will cross the phase barrier in a two-phase electrophoretic system from the preferred to the non-preferred phase.

Background

Protein Separation Techniques

There are many techniques that can be used to separate a desired protein from a solution. Although the technique that is examined in this project is electrophoresis of a two phase system it is good to have a basic understanding of some of the other methods that can be used. Some of these methods include affinity chromatography and hydrophobic interaction chromatography.

Affinity Chromatography is one method of selectively isolating and purifying enzymes and other important macromolecules. The process involves the protein being passed through a column that contains a gel or polymer that special competitive inhibitors or ligands have been covalently attached. (Cuatrecasas, 1970) The idea is that by selecting a proper ligand the protein can be either retarded by it or just pass through allowing a collection of the desired protein at the bottom of the column.

Hydrophobic Interaction Chromatography (HIC) is another method that can be used for protein separation. In HIC the hydrophobic regions that most proteins have are exploited to force separation. The separation occurs because the proteins hydrophobic surfaces are reversibly bound to hydrocarbon tails or aromatic rings that are immobilized in stationary micro porous matrix. (Cummins & O'Connor, 2011) Steps are then taken to remove the proteins from the bonds in a such a way as to purify the protein that is desired.

Electrophoresis

Electrophoresis is a process by which particles dispersed in a fluid move under the influence of an electrical field relative to the fluid. The process works via the exertion of an electrostatic Coulomb force on the dispersed particles by the electric field. This columbic force is generated because the dispersed particles have a surface charge that interacts with the electric field moving through the fluid. It is important to note while the particle does have a surface charge the electricfield is actually not directly interacting with the particle; instead it is exerting a force on a diffuse layer of charges that surround the particle. While sitting in solution prior to the application of the electric field the charged particles will attract charges of the opposite polarity from the fluid; these charges form a cloud that surrounds the particle. When the electric field is applied this cloud of charges shield the particle from the field, instead they are pushed along by the force exerted by the electric field which pulls the particle along with it through viscous stress. This movement of the particle and its surrounding charge cloud is resisted by the viscous friction force present within all fluids and the electrophoretic retardation force which is caused by the small amount of electric field that penetrates the charge cloud and exerts a force on the particle in a direction contrary to the movement of the charge cloud.

The electric field is generated by passing a current through the holding fluid. In order to properly conduct a current it is necessary to use a containing fluid with spare charged particles available, in order that they can form the charge cloud that surrounds the dispersed particles. This condition can be satisfied by using a buffer solution, though if this is the case careful consideration on solution pH must be made when the dispersed particle is a protein. Depending on the pH of the solution the protein will exhibit different net charges; this is related to the isoelectric point of the protein. The isoelectric point is

a pH level specific to each protein where it will exhibit a net zero charge, below this pH the protein will exhibit a negative charge while above the isoelectric point it will have a net positive charge.

The aqueous two-phase system is formed by mixing two water-based, immiscible substances. Consequently, when the limiting concentrations of polymers in the mixture are exceeded, the two phases composed of water and non-volatile components are formed. Since the limiting concentrations depend on the molecular weight, pH, temperature and ionic strength of the components, the separation into two phases is therefore affected and determined by these factors. For example, lowering the temperature of homogenous solution makes phase separation energetically favorable. (Smolders, Aartsen, & Steenbergen, 1971)

According to Smolders et al there are essentially two major types of liquid-liquid phase separation varying in the mechanism as well as in the final state of separation. The "Nucleation and Growth" mechanism, in which the solution exhibits a behavior similar to the pattern known from liquid-gas separation, where the solution would eventually become a dispersion of droplets of one of the equilibrium phases in the other one. This process is based on crystallization kinetics and morphology of polymer crystals growing in the solution and is expected to result in a more or less rigid polymer rich mass with solvent-filled holes, or two liquid layers, one almost pure solvent and the other polymer rich. Smolders notes that this sort of phase separation easily occurs for polymer concentrations higher than a few percent, since this condition allows for an easily obtainable undercooling below the binodial curve, which is essential to this process. (Smolders, Aartsen, & Steenbergen, 1971)

Another phase splitting mechanism depends on the equilibrium thermodynamic properties of liquid-liquid phase separation, the mechanism called the "Spinodal Decomposition". This type of separation is caused by the instability of the solution to even the smallest fluctuations in concentration. This theory, given by Cahn indicates that these small fluctuations would increase in amplitude with time in the early stages of the process, but if this pattern is conserved, the polymer-rich regions would increase in viscosity. The morphological structure expected from this sort of mechanism is a more or less rigid mass consisting of interconnected regions of the concentrated polymer phase, embedded in the dilute polymer phase (practically pure solvent). If the polymer-rich has sufficient mobility, the regions can eventually split up into bulk liquid phases. (Smolders, Aartsen, & Steenbergen, 1971)

The investigation of polyethylene glycol (PEG)-dextran solution is one of the most widely studied such systems. In this particular system the phase formed by the more hydrophobic PEG has a lower density than the bottom dextran-rich hydrophilic phase with the interface layer in between the two. The difference in affinities between the two phases affects the phase separation and allows for protein/enzyme partitioning into one of the phases. In fact, the PEG-dextran system is known to be used for protein purification because of its high water content in both phases (70-90% w/w) and a low interfacial tension, but with a drawback of a high cost of the purified dextran used. (Chaplin, 2004)

Theoretical Model

Electrophoresis of aqueous two-phase system has been numerically modeled by Clark and Lindbald in a 2D model based on the previous single-dimensional numerical model made by Levine and Bier. Demonstrating the electrophoresis in a flow device is very challenging because the concentration of solute and its position in time depends on multiple variables including electric field strength, mobility and phase partitioning and because the electrostatic potential and pH can be affected by an uneven distribution of buffer ions. (Clark & Lindblad, 2011) Therefore Clark used a dilute solution with a constant pH, temperature, electric field strength and constant excess of buffer ions in each phase, as well as an assumption of equilibrium at the phase interface to create a simple representation of his and others' experimental results. The model was created in COMSOL 3.5 simulation software using Navier-Strokes equations, a series of equations involving solute diffusivity, mobility, partitioning coefficients, and time steps and element mesh modifications for more polished results.

Clark compared his numerical results to the model made by Levine and Bier as well as to the experimental results obtained by Levine and Bier using a U-tube, Clark and Lindbald using a flow system, Clark and Marando using a batch system, and Munchow et al using a microchannel flow system.

The obtained model exhibited a buildup of solute at the phase interface as solute migrated from preferred phase on the bottom to non-preferred phase on the top as Levine stated. Extending to the longer time, however, the electrophoresis is reduced and at higher electric field strength the solute starts to cross the interface. The protein moves to the non-preferred phase, even though polarization occurs, as opposed to the results indicated by Levine model and experiment. Clark attempted to simulate Munchow experiment using the model to show the behavior the behavior of the solute in the microchannel environment. It showed a buildup of solute near an anode in low flow boundary layer near the wall at high electric field, which was probably not seen by Munchow because they stopped increasing the field due to mixing at the interface, which causes polarization, but at high electric field the effects would diminish. (Clark & Lindblad, Numerical Analysis of Two-Phase Electrophoresis, 2011)

The model made by Clark at least qualitatively describes the experimental results acquired by Clark-Lindbald in the flow system, and Clark-Marando in the batch system. Clark claims that the reason that Levine and Bier showed no or little solute migration to the non-preferred phase must be other than the effects of phase partitioning thermodynamics. He concluded that the electrophoresis in an aqueous two-phase system produced polarization effects at the phase interface, which increase with an increasing the applied electric field strength. The polarization effects do not affect the separation if the solute does not have a strong preference for either phase or if the electric field strong enough to overcome partitioning preferences. Therefore the separation can be achieved with a strong electric field perpendicular to the phase interface and well balanced partitioning, flow and electrophoretic effects. (Clark & Lindblad, Numerical Analysis of Two-Phase Electrophoresis, 2011)

Based on its success in demonstrating the electrophoresis in a two-phase system it was decided that Clark's model would be a good representation of our U-tube two-phase system and it served as a basis to our predictions and evaluation of the system.

Procedures

Experimental Equipment

A variety of equipment was used in the course of experimentation. A brief review of the equipment used, how it was used and the reasoning behind the design of various apparatus is outlined in this section. In modeling the U-tube electrophoresis experiment three different U-tube apparatuses were constructed with internal diameters of 5 mm. The actual tubes were all 1 mm wall clear glass that was bent using direct heat from a Bunsen burner. Three different geometries of tube were selected in order to conduct different experiments types.

Large U-Tube

The first U-tube was designed to most accurately mimic the experiments performed by Levine and Bier; it had 34 cm legs with a bend radius of 8 cm. The first u-tube presented issues during experimental trials due to the large distance of 97 cm between the electrodes; this resulted in heating of the solution and degradation of current during trials. Solution heating caused apparent protein denaturation, observed as the formation of precipitated protein granules. Current degradation was observed by keeping a log of the current readout from the Bio-Rad 3000xi power supply. It was theorized to be an issue because the current is the driving force behind the protein migration, and loss of current would conceivably cause a corresponding reduction in protein migration velocity.

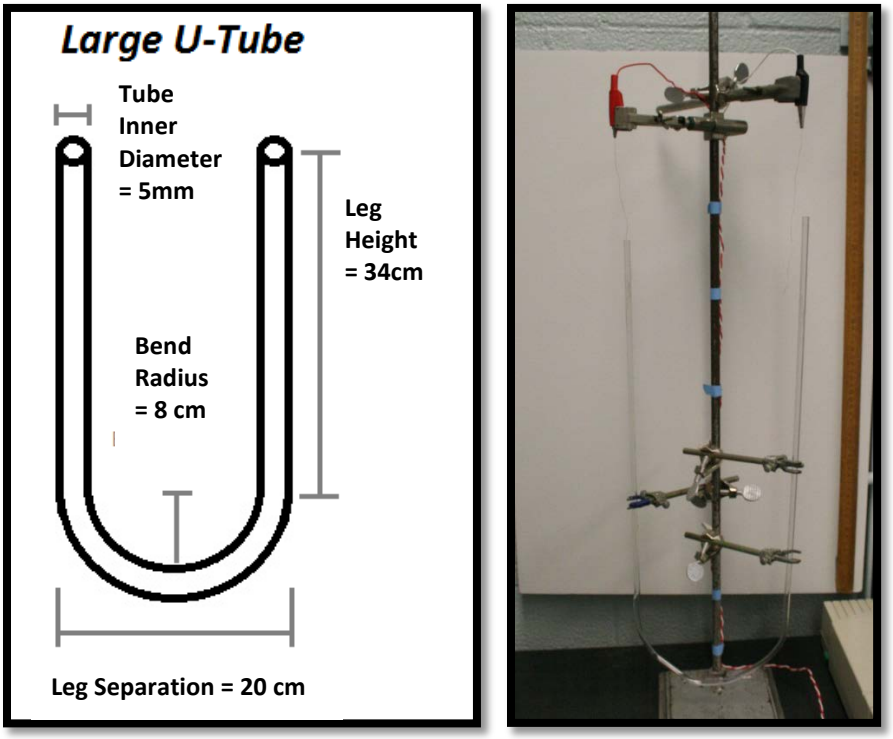

Figure 3: Large U-Tube Information and Picture

Short U-Tube

A modified U-tube was then built to overcome some of the issues faced by the first; this smaller U-tube had 12 cm legs with a bend radius of 7 cm. The smaller size of the U-tube allowed for it to be placed in an ice bath, potentially limiting the effect of solution heating and the resultant protein denaturation. Additionally the shorter length between the electrodes (44 cm) allowed the current to remain consistent throughout trials.

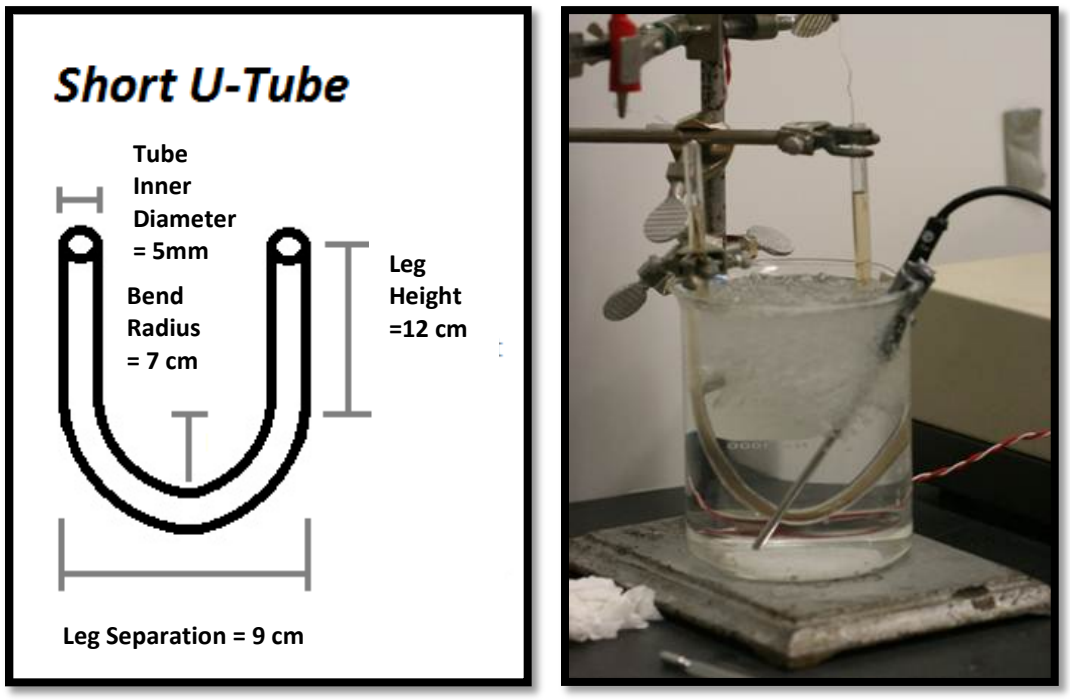

Figure 4: Short U-Tube Information and Picture

Straight U-Tube

In order to observe the behavior of applied electric currents on the single phases of the solutions prepared for the two phase trials a third U-tube was bent. This U-tube was dissimilar to the others in that it consisted of two small radius (2 cm) ninety degree bends with short 1.5 cm vertical legs and a 14.5 cm straight leg joining the bends. This 'straight' U-tube had the smallest electrode separation (19 cm) which allowed for the highest current for each solution.

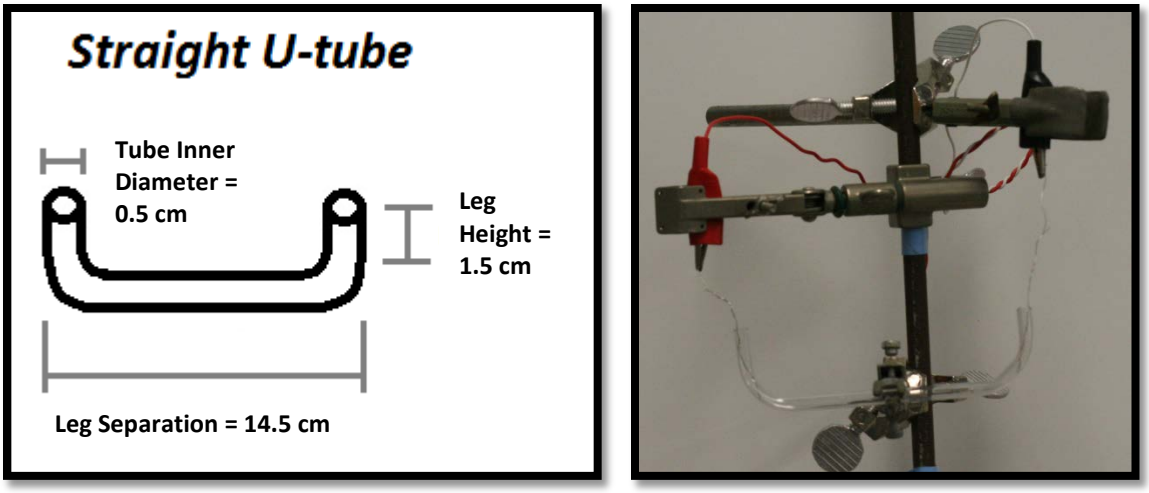

Figure 5: Straight U-Tube Information and Picture

Power Supply

The same power supply was used for all trials; the Bio-Rad 3000xi. This power supply is programmable to run at either constant voltage, current or power. The power supply was able to generate a high maximum potential of 3000V. The desired operation was 1mA constant, with voltage varying to maintain the current. Unfortunately, in many trials this was not possible because as the protein migrated so did the buffer ions, increasing the internal solution resistance. As a result the power supply was often set to run in constant potential operation just below the maximum potential, and current was observed through the experiment. The microprocessor control equipment in the Bio-Rad 3000xi provides for very accurate measurements of applied currents with a reported voltage set point accuracy of +/- 1% from 500V-3000V (this range includes the typical operating conditions) and a current set point accuracy of +/- 3mA in the 1mA-100mA range. (Bio-Rad Laboratories) Since the power supply unit was mostly run in the constant voltage operation mode, the accuracy of measured electrical strength is rather accurate at +/- 1%.

Due to limited information in the production literature there was some uncertainty in determining which electrode was the cathode, and which electrode functioned as the anode. This is an important consideration, because it is necessary to know which electrode the protein migrates towards in order to determine the nature of the actual separation. It is important to note that an electrophoresis system is best compared to a capacitor where the two electrodes are the charged plates and the solution in between represents the dielectric (electrical insulator). Of these two plates the anode is the positively charged electrode, through which an electrical current enters a circuit. Conversely the cathode is the negatively charged electrode in electrophoresis systems, since the cathode emits electrons which contribute to a negative current.

In order to empirically determine if this understanding was accurate an experiment to determine which electrode is actually the cathode and which is the anode was performed. A multimeter was connected between the labeled positive electrode, which was assumed to be the anode, and the labeled negative electrode. A positive conventional current (conventional current refers to the convention that current

flows in the opposite direction as the electrons) was measured with the ammeter, indicating that the electrode labeled as positive was in fact the anode, and the electrode labeled as negative was the cathode.

Preparation of Two Phase System Solutions for Experimentation

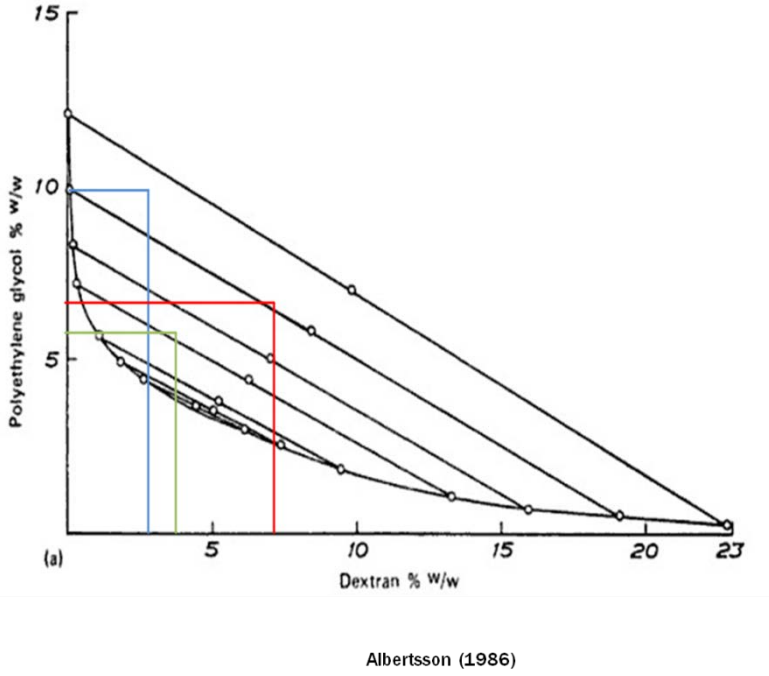

Figure 6: Phase Diagram for Dextran 500 – PEG 8000 at 20 °C

The phase diagram in Figure 6 was used to determine the amounts of dextran and PEG to use to create the solutions described below.

Solution 1

The first solution we prepared in order to run an electrophoresis experiment was prepared on February 17th, 2011. The first step was to insure that all of the lab equipment was clean including three empty 400 mL beakers, a 400mL Erlenmeyer flask, two lab spatulas, a small lab spatula, a magnetic stir bar, a glass stirring rod, a graduated pipette, and three weigh boats.

A concentrated solution of pH 9 was made in the Erlenmeyer flask by adding Trizma base, with a molecular weight of 121.1, to Millipore water. The pH was determined using an Accumet 950 pH meter. Once the pH held steady at 9 the concentrated solution was labeled “Conc. pH 9 Solution” and set aside to be used later.

The mass balance was then zeroed with one of the empty weigh boats. Twenty grams of polyethylene glycol (PEG), with a molecular weight of 8,000, was then weighed out. The twenty grams were to be ten weight percent of the final solution. The weigh boat was then set aside on the lab bench,

The mass balance was re-zeroed with the second empty weigh boat. Six grams of dextran, with a molecular weight of 500, were then weighed out and set aside with the PEG. The six grams being three weight percent of the final solution.

The weigh boats of PEG and dextran were then emptied into one of the clean 400 mL beakers. One hundred and sixty four milliliters of Millipore water was then added to the beaker with a graduated pipette. 164 mL of water were added because water weighs one gram per milliliter and the Millipore water was to be eighty seven weight percent of the solution. The PEG and dextran were mixed into solution using a Spin Master mixing plate and a magnetic stir bar. Any clumps of particulates that formed on the top of the beaker as it was mixing were broken apart with a glass stir rod.

After the solution was well mixed the pH was brought up to nine by adding a few drops of the concentrated pH 9 solution mixing and then checking the pH with the Accumet pH meter until the pH had risen to nine and was steady.

The well mixed solution of PEG and dextran with a pH of 9 was then set aside on the lab bench for later. The mass balance was re-zeroed with the final empty weigh boat. 0.2 grams of hemoglobin from bovine blood was then weighed out. 0.2 grams of hemoglobin were weighed out because the solution was 200 mL and the protein concentration was supposed to be one milligram per milliliter. The hemoglobin was then added to the 400 mL beaker containing the PEG, dextran, and Millipore water. The solution was again mixed with the Spin Master mixing plate and a magnetic stir bar.

Once the hemoglobin was mixed into the solution the stir bar was removed. The beaker was then sealed with parafilm and labeled “Solution 1” with the date. The concentrated pH 9 solution was also sealed with parafilm. The concentrated pH solution was placed in the fridge to be used when other solutions were to be made.

The sealed beaker with the solution was allowed to sit out for twenty four hours so that it would split into the two phases, the top phase being heavy with PEG, and the bottom dextran and the hemoglobin. The two phases were pipetted into the other two empty 400 mL beakers. The phase barrier and surrounding were discarded to remove impurities. The two beakers were labeled as “Solution 1 Top Phase (PEG)” and “Solution 1 Bottom Phase (DEX)” with the date of creation.

The two phases were then ready to be used in electrophoresis trials.

Solutions 2 & 3

Solutions 2 and 3 were prepared using the same procedure but with alternate values for the amount of PEG, dextran, Millipore water, and hemoglobin.

Solution 2 was made on February 20th, 2011 with 11 grams of PEG, 7.6 grams of dextran, 181.4 mL of Millipore water, and 0.1 gram of hemoglobin. The PEG is 5.5 weight percent, the dextran is 3.8 weight percent, and the Millipore water is 90.7 weight percent of the solution. The hemoglobin was added at a concentration of 0.05milligrams per milliliter for a total of 0.1 g of protein.

Solution 3 was made on February 22nd, 2011 with 12 grams of PEG, 14 grams of dextran, 174 mL of Millipore water, and 0.1 gram of hemoglobin. The PEG is six weight percent, the dextran is seven weight percent, and the Millipore water is 87 weight percent of the solution. The hemoglobin was added at a concentration of 0.05milligrams per milliliter for a total of 0.1 g of protein.

Solution 4

Solution 4 was made on February 28th, 2011 in order to perform a single phase experiment with a higher protein concentration. 25 mL of the top phase from Solution 2 was poured into a clean 50 mL beaker and set aside. The mass balance was then zeroed with an empty weigh boat. 0.02 grams of hemoglobin were weighed out then added to the beaker containing 25 mL of the top phase of Solution 2. The solution was then mixed with a glass stir rod until the hemoglobin had dissolved into solution.

Solution 5

Solution 5 was made following the same process as Solution 2 except the pH was raised to 11. The difference in pH caused a change in the preferred phase of the protein making the top phase more desirable.

Table 1: Solution Weights of Components

Solution	pH	Dextran (g)	PEG (g)	Water (g)	Protein (g)
1	9	6	20	164	0.2
2	9	7.6	11	181.4	0.1
3	9	14	12	174	0.1
4	9	**TOP PHASE OF SOLUTION 2**			0.02 Extra
5	11	7.6	11	181.4	0.1

Table 2: Solution Weight Percents of Components

Solution	pH	Weight % Dextran	Weight % PEG	Weight % Water	Protein (g)
1	9	3	10	87	0.2
2	9	3.8	5.5	90.7	0.1
3	9	7	6	87	0.1
4	9	**TOP PHASE OF SOLUTION 2**			0.02 Extra
5	11	3.8	5.5	90.7	0.1

Results

Theoretical Model

Table 3: Constants used for the numerical modeling of the two-phase electrophoresis system

Name	Expression	Value
cond	0.04	0.04
V0	200	200
R	8.314	8.314
T	298	298
D	6.8e-11	6.8e-11
Dt	D	6.8e-11
Db	D*0.34	2.312e-11
cb0	0.2	0.2
ct0	0.008	0.008
M	10000	10000
K	1	1
char	-20	-20
mut	Dt/(R*T)	2.744623e-14
mub	Db/(R*T)	9.331717e-15

The theoretical model of the protein separation in the two-phase, U-tube system, was created in COMSOL 3.5. The geometries used were: electro-kinetic flow and conductive media DC along with the constants in Table 3. The model assumed initially no protein present in the top phase (PEG-rich phase), interface K value as 1, as well as a uniform concentration of buffer ions and a constant pH 9 throughout both of the phases at all times. This simplified model allowed us to run it first in respect to electro-kinetics and then, based on those results with respect to concentration.

The system ran for 3600 seconds at the specified conditions, with the appropriate constants as shown in Table 3, and mesh, as determined by running the model several times until the image presented all the important aspects.

The initial image consisted of white PEG-rich phase on top on both anode and cathode sides (indicating the lack of protein), and a solid gray coloring of the bottom dextran-rich phase (indicating a uniform protein concentration). When watching the recap of this separation process it was observed the coloring began to diminish in the bottom phase of the anode side, starting to become progressively more white right under the interface, and at the same time the top phase of the cathode side began to turn from white to gray progressively from the interface up, with the coloring becoming darker at the top once it reached the cathode. The final image (see Figure 6) showed a completely white anode side top phase, with a bottom phase being white right under the interface of the anode side and becoming darker the closer to the interface of the cathode side, being the darkest right under the interface, where the boundary of the top phase of the cathode side begins. The coloring above the interface is slightly lighter than right below it, but it gets darker the closer to the cathode itself.

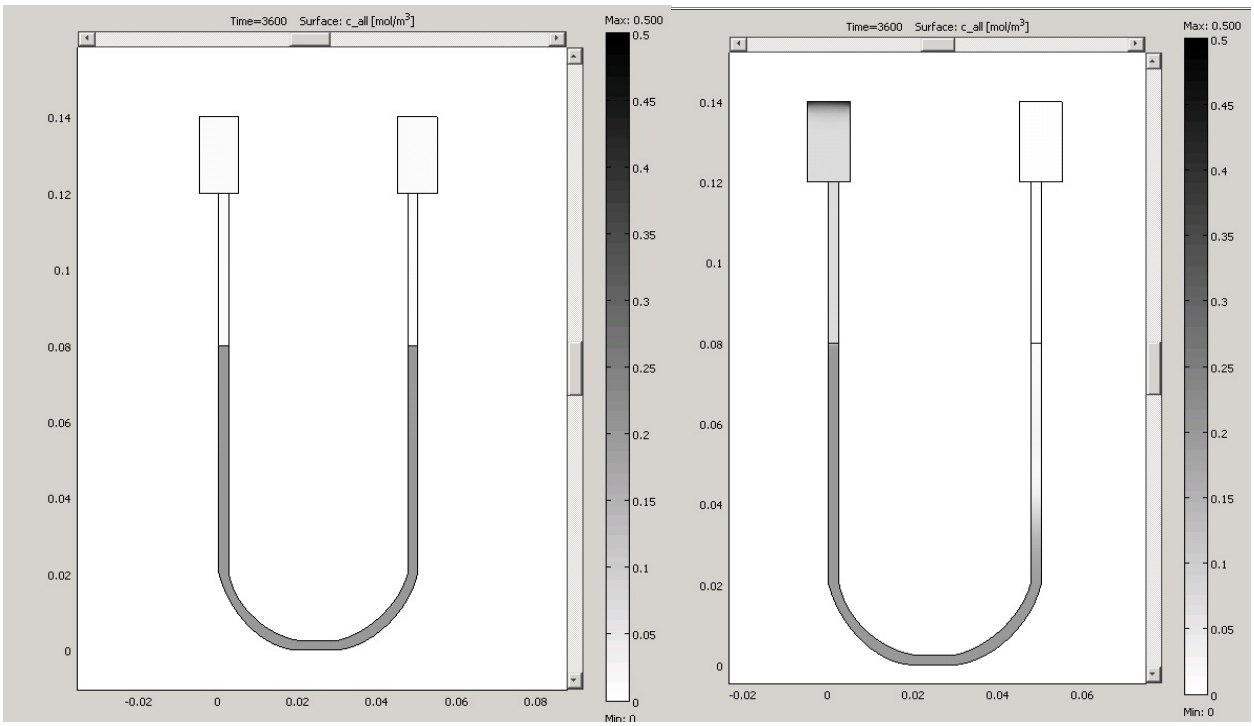

Figure 7: Initial (left) and final (right) image of an hour-long run with K=1

Since the coloring corresponds to the concentration of protein, in that the darker the coloring the higher protein concentration, the model showed that theoretically the protein should move away from the cathode towards the anode. While crossing the interface, protein would accumulate right below, possibly as a result of lower viscosity of the bottom phase in relation to the top phase. Nevertheless, the model successfully proved that protein would make its way across the interface and migrate towards the anode.

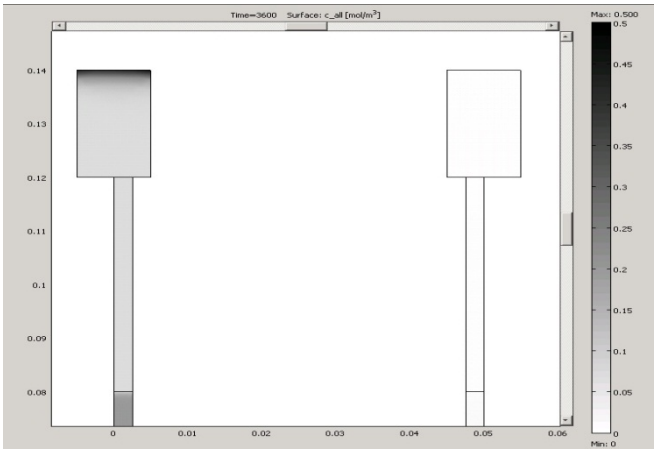

Figure 8: Close-up image of the top phase of the run with K=1, after an hour

To check the validity of Levine and Bier theory that there would be no or little migration of the protein across the phase interface into the non-preferred phase at low partition coefficients, we ran the model with a constant of K=0.1 as well as K=2. At K=2 protein move across the interface and towards the top

much faster than at K-1. Although at K=0.1 a temporary holdup of protein was noticed right at the phase interface, as seen on the graph in Figure 8, but while the experiment ran for an hour that holdup vanished and the protein moved up to the top of the non-preferred phase.

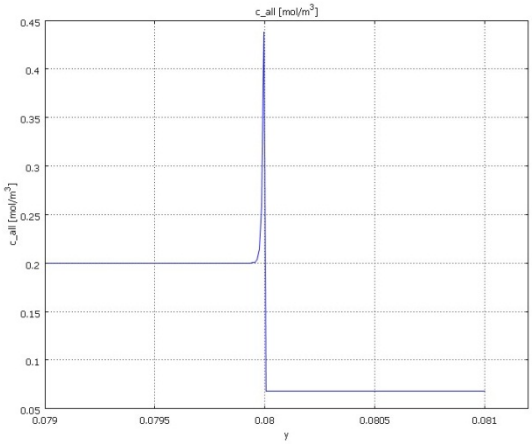

Figure 9: Concentration gradient graph across the interface of the run at K=0.1

Based on the above models it was concluded that even though Levine and Bier were right in that there is a holdup of protein at the interface at low partition coefficients, if the experiment is run for an extended time the electrophoresis is reduced and also if the electric field strength is increases, the protein does move across the phase interface and migrates to the top. Therefore the final conclusion was that even though polarization might occur in a two-phase electrophoresis system, its effects do not interfere with the separation of the protein if the protein does not have a strong preference for either phase or if the electric field strength is strong enough to overcome these preferences.

Results and Discussion

The following section serves as a review of each of the individual trials conducted in testing electrophoresis of proteins in two-phase polymer solutions. Pictures of important observations are included to illustrate in more detail those observations. Additionally data for the setup of each experiment is provided, along with brief discussions of each trial.

Trial 1

The first experimental trial was designed to replicate the U-Tube two phase polymer electrophoresis experiment of Levine and Bier using the solution compositions outlined by Clark and Marando. Levine and Bier predicted that the protein would concentrate and begin to migrate towards the anode, but the migration would be held up at the interface between the two polymer phases (denoted the interface). Contrarily *Two-Phase Electrophoresis of Proteins* and initial COMSOL modeling predicted that this inhibition would only be temporary. (Clark & Marando, 1993) The large U-Tube was used to mimic the equipment used in *Electrophoretic Transport of Solutes in Aqueous Two-phase Systems*. (Levine & Bier, 1990)

Date of Trial: February 21st, 2011
Solution: Solution 2
Apparatus: Large U-Tube
Power Supply: Bio-Rad 3000Xi

Maximum Potential	*2000 Volts*
Maximum Current	*1 mA*
Maximum Power	*30 W*
Constant Potential	*1500 Volts*
Anode Position	*left*

Figure 10: Solution 2 Before Separation: Both phases have similar physical properties

Initial Observations

Compared to the first solution prepared, solution 2 exhibited a much more even distribution of protein in the top and bottom phases (Figure 10). Additionally the viscosities of the phases appear to be made similar to one another compared to solution 1. This can be explained by the phase diagrams in *Two-Phase Electrophoresis of Proteins*, since the position of the solution in these diagrams is much closer to the 1.0 partition coefficient there is more even distribution of protein between the phases. (Clark & Marando, 1993) Upon filling the U-Tube apparatus both phases separated cleanly with a mildly distinguished interface. As a note many of the pictures in this section had their exposure adjusted to better reveal color differences because of a limitation in the

Figure 11: Observation 1 Anode and Cathode Interphase: Anode interface (left) displays a clear region, while cathode (right) exhibits a dark band

photography equipment used during this trial.

Observation 1 – 10 minutes

At the first observation point activity at the interface was discovered. On the anode side a clear band formed in the former position of the interface between the top and bottom phases (Figure 11). The cathode interface exhibited opposite behavior with the generation of a dark band at the interface. The dark and light regions in the solution respectively represent areas of high and low protein concentration; this standard remains consistent throughout all trials.

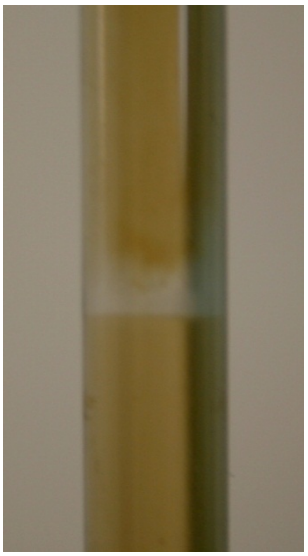

Figure 13: Observation 2 Anode Interphase: Expansion of clear band at the interface

Figure 12 - Observation 2 Bottom Phase: Formation of a diffuse protein cloud under the anode interface

Observation 2 – 20 minutes

At the second observation point there was limited activity on the cathode side of the U-Tube, while the anode side experienced extensive changes. The cathode interface exhibited the same behavior as in the first observation; the presence of a thin dark band at the immediate interface of the top and bottom phases. The anode interface had much more drastic changes. The light band at the interface expanded and took on a more diffuse appearance; it is interesting to note that the clear area was only visible above the interface and was sharply bounded at the interface (Figure 13). In the region below the interface dark currents of concentrated protein were observed (Figure 12). These currents formed unexpectedly and appear to be directed towards the cathode.

Observation 3 – 36 minutes

Continuing with previous trends at the third observation point there was continued activity at anode interface. As shown in Figure 14 the clear band above the interface remains but a diffusion pattern appears above the interface moving into the top phase. On the cathode side there was limited change since the last observation; there was still a dark band with limited diffusion. Additionally there was no observable activity at either electrode besides simple bubbling that was attributed to electrolysis of water. While all observations have noted migration of protein, the trend was not fully clear at this point in the experiment but there was a clear relationship between the protein migration and the interfaces.

Figure 14 - Observation 3 Anode Interphase: Clear band still present but it now exhibits a diffusion cloud

Observation 4 – 47 minutes

Figure 16 - Observation 4 Anode Interphase: Diffusion cloud has now moved under the interface

At the 4th observation point there was again limited activity at the electrodes on both sides, and very little change at the cathode interface. Similar to other observations periods the anode interface exhibited very radical behavior at the 4th observation. Whereas there was previously a clear band above the interface at this point the entire top phase had become clear, leaving a very diffuse region at the interface. Below this region were well defined protein currents moving into the bottom phase (Figure 16). This observation supports previous observations of protein migration towards the cathode. It was interesting to note though how all of this peculiar behavior was focused at the interface.

Figure 15 - Observation 5 Anode Interface: Diffusion of protein into bottom phase is much more prevalent and well developed

Observation 5 – 76 minutes

Observation 5 followed the trend of previous observations in that the only notable activity occurred at the anode interface. The cathode interface continued to exhibit a dark band at the interface, while the electrodes only bubbled. The primary change at the anode interface was further development of the diffusion pattern previously observed (Figure 15). The protein cloud observed at the anode interface had completely moved under the interface by the 5th observation, leaving a clearly defined top boundary. Additionally the diffusion cloud, the area of mixed higher and lower concentrations, stretched much lower into the bottom phase. This observation makes it very clear that the protein is migrating towards the cathode.

Figure 17 - Observation 6 Full U-Tube: Both interfaces can be seen near the top of the frame, the anode (left) appears clear above and dark below, while the cathode exhibits a dark band

Observation 6 – 96 minutes

The final observation point noted the continuation of previous trends. The anode side top phase continued to clear out, while the region below the anode interface darkened as the diffusion cloud became more prominent.

On the cathode side the dark band at the interface remained in place with similar darkness and diffusive characteristics (Figure 17).

Summary of Observations

The first trial of the electrophoresis experiments resulted with a few very important observations and conclusions. Clearly the most basic is that an applied electric field will result in migration of protein in solution. The general trend of this migration is for the protein to move towards the cathode electrode, as observed by the diffusion at the anode interface. Also while there was significant activity around and at the interfaces, neither the cathode or anode interface exhibited complete inhibition of protein migration. Particularly at the anode interface there was significant diffusion; beginning as a clear band above the interface as time passed a large cloud formed under the interface. It was clear this diffusion cloud was a result of the migration of protein through the interface because of the clear region above the interface, suggesting that the protein in the top phase migrated through the interface into the bottom phase. After the first trial it was clear that the electrical current will induce protein migration towards the cathode through both interfaces.

Trial 2

Trial 2 used solution 3 to observe any changes in protein behavior compared to trial 1 which used solution 2. The primary change between solutions 2 and 3 is that solution 3 used significantly more polymer, specifically PEG the bottom phase component. By increasing the concentrations of polymer in both phases the viscosity of each solution would increase, but the concentrations were selected to ensure that the partition coefficient of the solutions would be similar. Since the partition coefficients were similar there was only a limited change in which phase was favored, and any changes in activity would primarily be a result of the increased viscosity of the phases. The settings on the power supply were left the same to eliminate any effect of changed electrical field.

Date of Trial: February 23rd, 2011
Solution: Solution 3
Apparatus: Large U-Tube
Power Supply: Bio-Rad 3000Xi

Maximum Potential	*2000 Volts*
Maximum Current	*1 mA*
Maximum Power	*30 W*
Constant Potential	*1500 Volts*
Anode Position	*left*

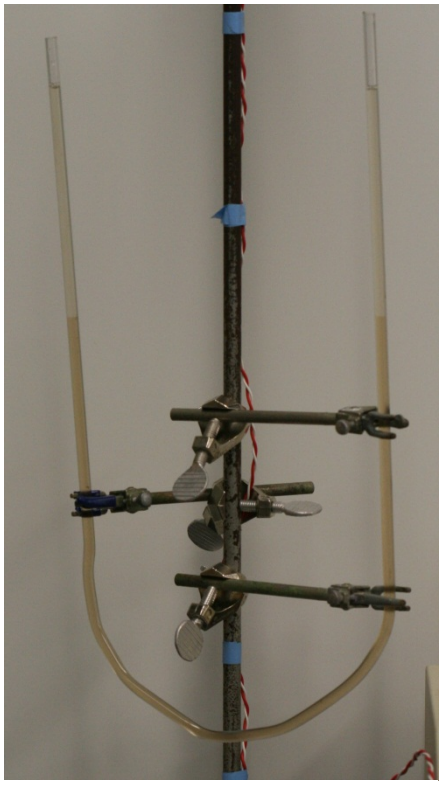

Figure 18 - Trial 2 Initial Observation Full U-Tube: Large color difference between the phases

Initial Observations

Upon settling after filling the U-Tube a few observations were taken. Notable was the color difference between the top and bottom phases (Figure 18). It was similar to the color difference in trial 1, showing the similarity in the partition coefficients between solution 2 and solution 3. Additionally the phase barriers were well defined, possibly as a result of the higher viscosities of both phases.

Observation 1 –29 minutes

Following an extended period of time of no activity besides bubbling on the electrodes, a more pertinent change was observed. Beneath the anode side interface a small concentration of protein formed on the right hand side (Figure 19). This concentration was observed because of its darker color than the surrounding solution in bottom phase. Of interest was that the top boundary of this protein concentration was at the interface, suggesting a potential inhibition to protein migration.

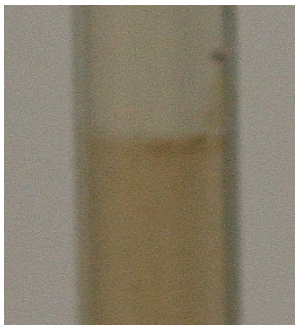

Figure 19 - Observation 1 Anode Interphase: Small concentration of protein beneath the interface

Observation 2 –40 minutes

At the second observation point additional darkening at both interfaces was observed. Shown in Figure 20 are both interfaces, thin dark bars at each interface correspond to the increased concentration of protein at these interfaces. Also of importance is the somewhat darker top phase on the cathode side.

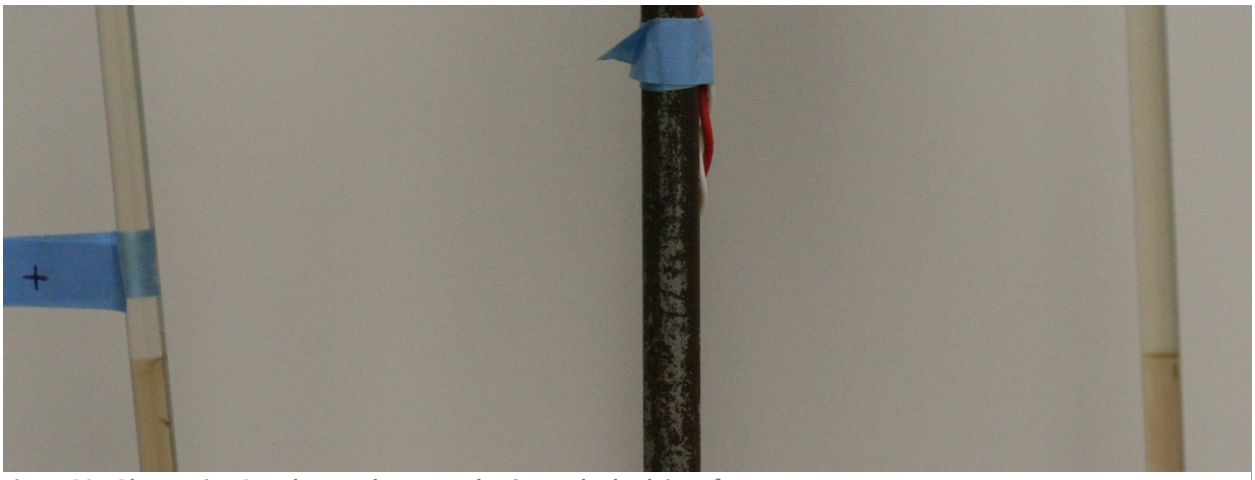

Figure 20 - Observation 3 Both Interphases: Darkening under both interfaces

Observation 3 –48 minutes

At the third observation point similar behavior was noted. Both interfaces exhibited darkening under the interface, possibly as a result of protein migration inhibition. Neither buildup of protein was significantly larger than in observation 2 but of note was the somewhat diffuse nature of both. On the anode side a small current of dark protein was observed moving from the interface down into the bottom phase (Figure 21). On the cathode side a clear band was observed immediately below the interface, but further below was a region of non-homogenous protein concentration, possibly migrated protein that had become held up at the interface (Figure 22). Additionally above the interface on the cathode side was a small diffuse region, apparently caused from the diffusion of protein through the interface.

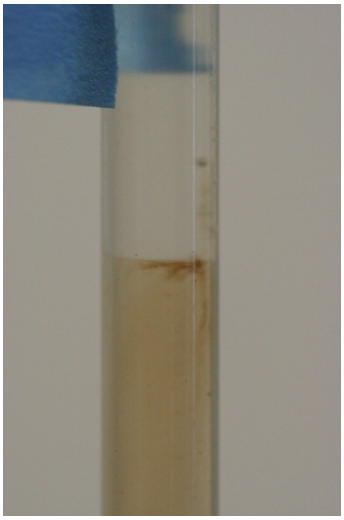

Figure 21 - Observation 3 Anode Interphase: Small current of protein observed below interface heading towards cathode side

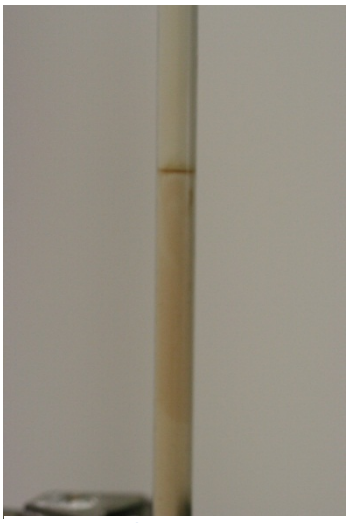

Figure 22 – Observation 3 Cathode Interphase: Diffusion through the interface and generation of non-homogenous region below

Observation 4 – 60 minutes

At the 4th observation point the previously observed behavior continued with bubbling at the electrodes and the majority of the activity occurring at the phase interfaces. The cathode interface displaced particularly interesting behavior with a continuation of what was noted at the third observation, just to a more extreme degree (Figure 23). The clear band became more defined, while the region below appeared even darker yet similarly heterogeneous as the previous observation. Immediately above the interface is a diffuse region that suggested that the interface was at most slowing, but not fully stopping the protein migration. At the anode interface there was somewhat contrary activity. Instead of darkening the interface appeared diminished and lighter. It seems that after the establishment of a local equilibrium the protein was able to migrate through the interface until the concentration in the top phase on the anode side began to decrease. As the concentration in the top phase decreased the concentration of the bottom phase which was in contact with the top phase at the interface experienced a corresponding decrease in concentration (Figure 24). Regardless of the contrary behavior of the concentration of protein at the two interfaces, they both exhibited migration through the interface.

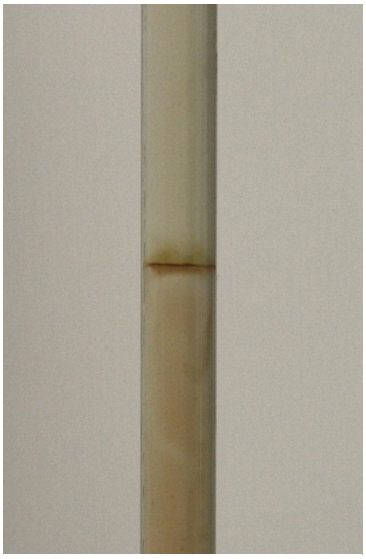

Figure 23 - Observation 4 Cathode Interphase: Dark band immediately at the interface with apparent diffusion through interface

Figure 24 - Observation 4 Anode Interphase: Clearing out of protein at the interface, apparent disruption of the interface equilibrium

Summary of Observations

Trial 2 was designed to test the effect of phase viscosity on apparent protein migration. Throughout the experiment a general migration trend towards the cathode was observed, mostly through the observation of protein currents under the anode interface and the selective darkening and lightening of the cathode and anode top phases respectively. Similar to trial 1 there was also current degradation throughout the experiment. Of particular interest was the behavior of the two interfaces. Summed up previously (in the observation 4 section) it was noted that initially both interfaces darkened, but then experienced different activity. The anode interface began to become clearer as time passed, corresponding with the lightening of the anode side top phase. On the cathode side the interface darkened, then became diffuse. A possible explanation is that as protein migrates towards the cathode it reaches the phase interface which has a particular concentration equilibrium dependent on the partition coefficient. This equilibrium is disrupted by the increased concentration of protein on one side, so the concentration on the other side increases to match. This new equilibrium is observed as the dark bands at each interface. As time passes the protein continues to migrate through the interface until, as was observed with the anode side top phase, one side of the equilibrium becomes depleted of protein;

once depleted the interface will clear out. This explanation relies on the assumption of a partial inhibition of protein migration at the interfaces, but not a complete stop.

Trial 3

The conditions used in trial 3 were designed to replicate the conditions in the Levine and Bier experiments. This was primarily achieved by using solution 1 which replicated the composition of the solution used in *Electrophoretic Transport of Solutes in Aqueous Two-phase Systems*. (Levine & Bier, 1990) The large U-Tube, based off of the design of the U-Tube in the Levine and Bier experiments, was used. Additionally it was originally intended to operate the power supply at the constant current mode at 0.1mA, but because of increasing resistance this was not possible, so instead the power supply was set to run at a constant potential of 1500 volts.

Date of Trial: February 24th, 2011
Solution: Solution 1
Apparatus: Large U-Tube
Power Supply: Bio-Rad 3000Xi

Maximum Potential	*2000 Volts*
Maximum Current	*1 mA*
Maximum Power	*30 W*
Constant Potential	*1500 Volts*
Anode Position	*left*

Initial Observations

Since solution 1 was used there was a large difference in the properties of each phase. The top phase is much clearer with an apparently lower viscosity. The large difference in physical properties of the two phases resulted in a very clearly defined interface (Figure 25).

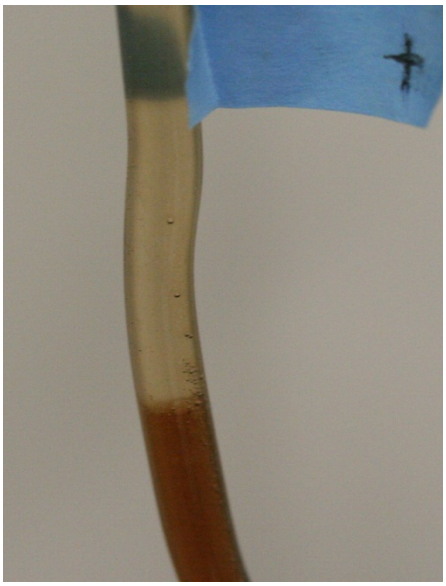

Figure 25 - Trial 3 Initial Observation of Anode Interphase: Very clearly defined interface

Observation 1 – 3 minutes

Immediately after the start of experiment a disruption at the surface of both interfaces was observed. Neither disruption was drastic enough to be noticeable in pictures at this point. Additionally both electrodes were bubbling.

Figure 26 - Observation 1 Anode Interphase: Slight disruption of interface

Observation 2– 33 minutes

At the second observation point similar behavior as the first observation was found. Both interfaces had undergone continued, slow disruption of the interface. Shown in Figure 26 is the diffusion of protein from the bottom phase into the top phase; while slight at this point the viscosity of the

bottom phase is conceivably a lot to overcome and cold be slowing any diffusion. Similarly on the cathode side the interface has become diffuse and no longer as clearly defined as it was at rest (Figure 27).

Figure 27 - Observation 2 Cathode Interface: Slight diffusion of protein at interface, no longer clearly defined

Observation 3 – 78 minutes

After a long period of limited change the protein rich bottom phase began to 'push' its way into the top phase on the anode side interface (Figure 28). It still appears that the viscosity of the bottom phase limits the migration of protein. The cathode side interface had similar inhibition to migration, apparently from the resistance to flow from high solution viscosity.

Figure 28 - Observation 3 Anode Interphase: Continued disruption of interface

Observation 4 – 93 minutes

At the 4th observation point a small globule of protein released from the disrupted interface and began to rapidly migrate (~1cm/12sec) towards the anode electrode. This is shown in the compound pictures in Figure 29.

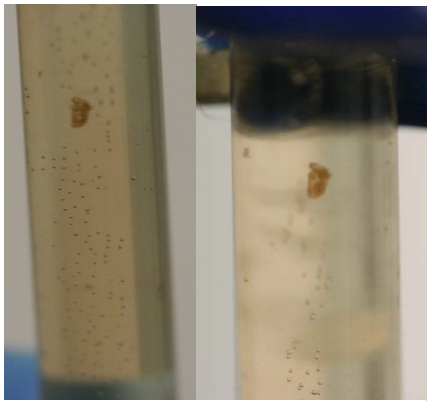

Figure 29 - Observation 4 Protein Release

Observation 5 – 120 minutes

By the time of the 5th observation the released protein had reached the bubbles above the anode electrode. No other protein was released from the bottom phase though. Despite the relative lack of change a darker cloud of protein formed under the anode interface. Shown in Figure 30, this cloud suggests the migration of protein towards the anode within the bottom phase.

Figure 30 - Observation 5 Anode Interphase: Formation of dark cloud under the interface

Summary of Observations

The most striking observation from trial 3 was the decrease in activity compared to trials utilizing other solutions. This is primarily a result of the high viscosity of the bottom phase of solution 1, which limits the ability for protein to migrate. Despite this limitation there was still an observed trend of protein migration

towards the anode electrode. It is possible that the interface could have been the primary inhibitor for this migration.

Trial 4

Trial 4 was setup as a repeat of trial 3 at a higher potential in order to observe the effects of increased electrical power. By increasing the constant potential difference between the two electrodes the current flowing through the solution will increase proportionally. In order to eliminate other variables the large U-Tube was again used with a fresh sample of solution 1. The electrical potential was raised from 1500 volts to 2950 volts, resulting in a 97% increase in current.

Date of Trial: February 25th, 2011
Solution: Solution 1
Apparatus: Large U-Tube
Power Supply: Bio-Rad 3000Xi

Maximum Potential	*3000 Volts*
Maximum Current	*5 mA*
Maximum Power	*35 W*
Constant Potential	*2950 Volts*
Anode Position	*left*

Initial Observations

Similar to trial 3, at initial observation solution 1 exhibited very distinctly defined phases with the top phase being far lighter in color and lower in viscosity than the bottom phase. The interface was again very well defined due to the vast difference in physical properties of each phase.

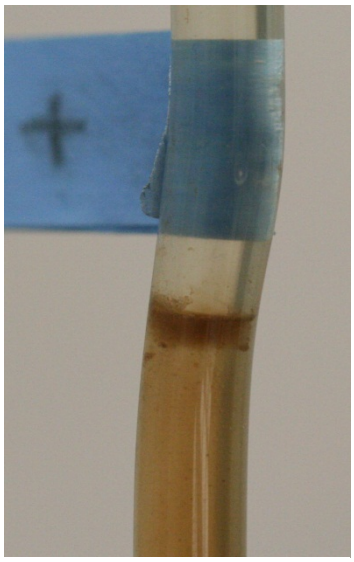

Figure 32 - Observation 1 Anode Interphase: Immediate formation of dark region below interface

Observation 1 – 11 minutes

Upon applying the now stronger electrical current to the solution there was immediate activity on the anode side of the U-Tube. At the anode interface a darkening occurred under the interface into the bottom phase (Figure 32). This darker region formed much more quickly than in previous experiments, suggesting that the increased current had a stronger effect on protein migration. This dark region is mostly homogenous, and begins sharply at the interface, though it becomes diffuse as it moves deeper into the bottom phase. Additionally an accumulation of protein formed in the bottom phase of the solution towards the anode side (Figure 31). This very dark region represents a region of very high protein concentration. Interesting to note was the region of the solution immediately before the accumulation to the leading edge of the dark band under the

Figure 31 - Observation 1 Protein Accumulation: A dark region of protein formed quickly after the application of electrical current

anode interface. It appears lighter than the at rest bottom phase, suggesting that protein has migrated from that region of solution towards the protein accumulation. Immediately this observation established the migration behavior of the protein in solution towards the cathode. Also of interest was the heat expelled by this protein cloud. The U-Tube glass immediately surrounding the protein cloud was significantly warmer to the touch than other parts of the glass. The formation of this accumulation also corresponded with a drop in current from roughly 0.85 mA to 0.45 mA; this current degradation was observed in all other trials.

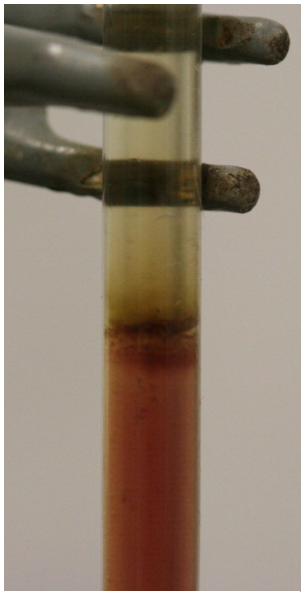

Figure 33 - Observation 2 Cathode Interphase: Formation of a darker region at the interface that appears to be diffusing through the interface into the top phase

Observation 2 – 23 minutes

Continuing with the increased activity previously observed the second observational period noted continued vigorous activity. The anode interface exhibited roughly the same behavior as in observation 1, with the presence of a dark band beginning at the interface diffusing into the bottom phase. More striking was the changes at the cathode interface, which was previously dormant. At the second observation point the cathode interface exhibited a very varied nature, with a dark region immediately below the interface, then a clear band right where the interface was previously (Figure 33).

Figure 36 - Observation 2 Protein Accumulation: The protein accumulation continued to rapidly migrate further into the bottom phase towards the cathode

Figure 35 - Observation 3 Protein Accumulation: The protein cloud continues to move deeper into the bottom phase

Above the interface was another dark region that appeared to be diffusing into the top phase. This seems to support the previous observation of protein migration towards the cathode. Also of note was the continued rapid migration of the protein accumulation deeper into the bottom phase towards the cathode. It is clear even this early into the experiment there was a migration trend towards the cathode at an increased rate. Current degradation continued, with current dropping to 0.35 mA at this observation point.

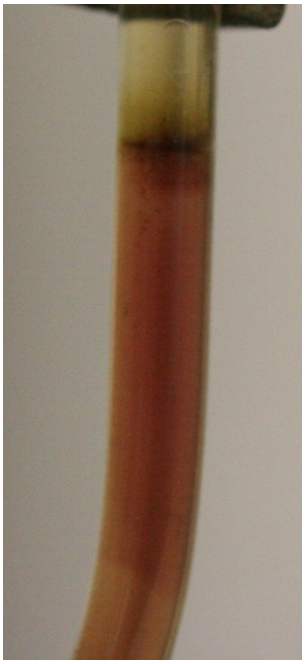

Figure 34 - Observation 3 Cathode Interphase: Continued diffusion of protein through interface

Observation 3 – 35 minutes

While the changes in the experiment since the 2nd observation are not as drastic compared to the changes from the 1st to 2nd observation there is still high activity. The region with the least activity was the anode interface, which continued to exhibit a dark band under the interface diffusing into the bottom phase. Deeper into the bottom phase the protein accumulation continued to migrate towards the cathode (Figure 36). Whereas at the second observation point the bulk of the protein was located at a particular pinch in the radius of the bend of the U-Tube (Figure 35) and the 3rd observation the majority of the protein had migrated past this point (Figure 34). Interesting to note was the trail of protein on the top wall of the U-Tube trailing behind the protein cloud. The clear region behind this cloud also expanded, it appeared to be following the trailing edge of the protein cloud. Additionally the cathode interface displayed some familiar, as well as unfamiliar behavior. Similar to observation 2 there was a dark band both immediately above and below the interface, with the dark band above the interface apparently diffusing into the top phase (Figure 37). The new behavior that was observed was the development of a large slightly darker region. While not as dark as the migrating protein cloud or the bands at the interfaces, a large region formed below the cathode interface and ended sharply roughly two centimeters below (Figure 37). By the third observation point current dropped to 0.2 mA, while not as drastic of a drop in current as other observational periods it is still significant and represents increasing solution resistance.

Figure 37 - Observation 4 Cathode Interface: Dark region below interface now appears to be two normal regions separated by a clear region

Observation 4 – 47 minutes

At the 4th observation point very similar behavior was observed as compared to the 3rd observation point. The anode interface was roughly the same, with a dark band below the interface that exhibited diffusion into the bottom phase (Figure 38). The protein accumulation in the bottom phase continued to migrate, but a vastly decreased rate. Shown in Figure 38 is the entire bottom phase of the experiment; the dark cloud of protein is located on the left near the bottom of the bend radius. The trail of protein on the top wall of the tube was still present as well as the clear area between the anode interface and the trailing edge of the protein cloud. The color contrast between this region and standard bottom phase on the right can be seen. At the cathode

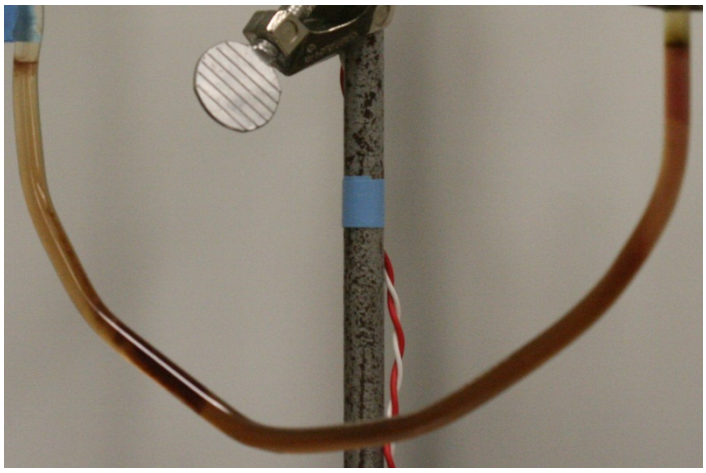

Figure 38 - Observation 4 Bottom Phase: Protein cloud continues to migrate towards the cathode electrode

interface the dark region below the interface no longer appears to be a concentrated region, rather it is standard bottom phase separated by a region of lower concentration (Figure 38). This could suggest the migration of protein near the interface towards the cathode with a slight inhibition at the interface causing a buildup of protein immediately before the interface. The clear area would represent a portion of the bottom phase which has undergone electrically induced protein depletion. Additionally current continued to drop, reaching an average value of 0.15 mA at this observation point.

Observation 5 – 97 minutes

After an extended period of familiar activity (protein cloud migration towards the cathode) with limited changes at the interfaces another observation was taken. Figure 39 shows the entire bottom phase of the experiment; there are obvious similarities with the interface activity as compared to Figure 38. The primary change from the 4th observation is the new position of the protein accumulation in the bottom phase and the growth of the clear band under the cathode interface. Both of these behaviors correspond with the observation of protein migration towards the cathode. By this point in the experiment the current degradation has stopped and the current has leveled off at 0.1 mA.

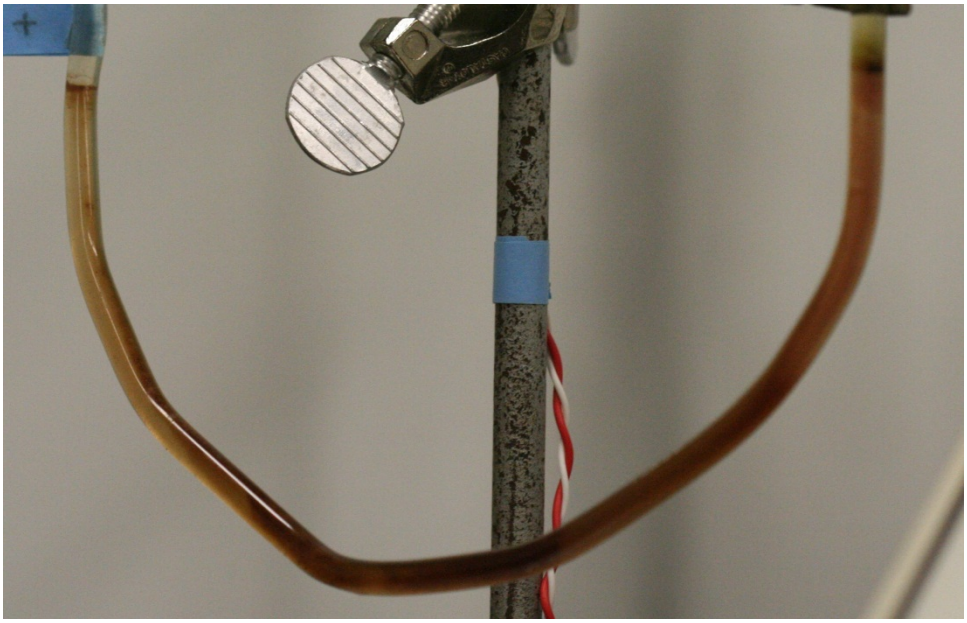

Figure 39 - Observation 5 Bottom Phase: Protein accumulation continues to migrate deeper into the bottom phase towards the cathode, clear band under cathode interface has grown

Observation 6 – 174 minutes

Following another long period of consistent behavior a final observation was made. Because of the stagnant nature of all activity zones at this point this was the final observation. Figure 40 shows the final profile of the bottom phase, with the trial typical dark bands at the interface, protein collection in the bottom phase and clear area behind the protein accumulation. By this point in time the clear band under the cathode interface began roughly where the protein accumulation terminated. The most interesting change is the location of the protein accumulation, which sometime previously began to migrate up the cathode side of the bottom phase. After beginning this migration it halted roughly 9

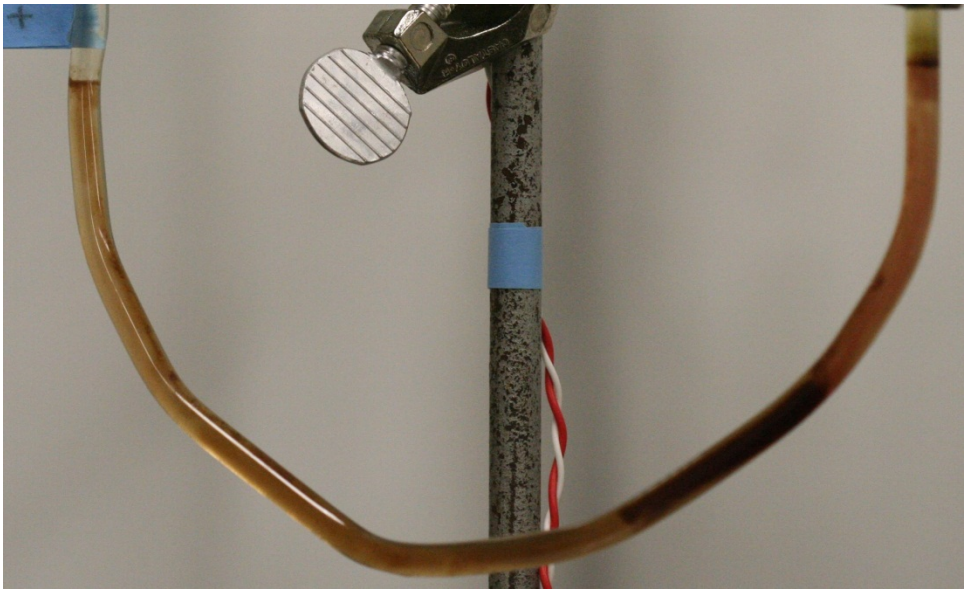

Figure 40 - Observation 6 Bottom Phase: Protein accumulation began to migrate up the cathode leg of the U-Tube but halted movement

centimeters from the tip of the cathode electrode tip. It is possible the protein denatured and became particulated and the effects of gravity on the suspended protein were too strong for the electrical force to overcome. Current had remained constant at 0.1 mA since the last observation.

Summary of Observations

The primary goal of trial 4 was to investigate the effect of increased electrical current on protein migration via a comparison to trial 3. The most obvious effect was what was predicted; the increased electrical current greatly increased the rate at which the activity zones (interfaces and bottom phase) exhibited changes. Almost immediately after the application of electrical there was formation of the characteristic dark bands at each interface, along with strong diffusion trends. A protein accumulation also formed shortly after applying the electrical current on the anode side of the bottom phase. This accumulation rapidly migrated deeper into the bottom phase towards the cathode electrode. The formation and concentration of this cloud of protein corresponded to a heating of the glass of the U-Tube surrounding the accumulation as well as degradation in current. Since current degradation was observed in other trials it was more carefully observed in this trial. Using Ohm's Law a rough correlation (since Ohm's Law is an experimental correlation and not a physical law the calculated resistance values are at best an estimate) of solution resistance was formed and plotted in Figure 41. The most important observations

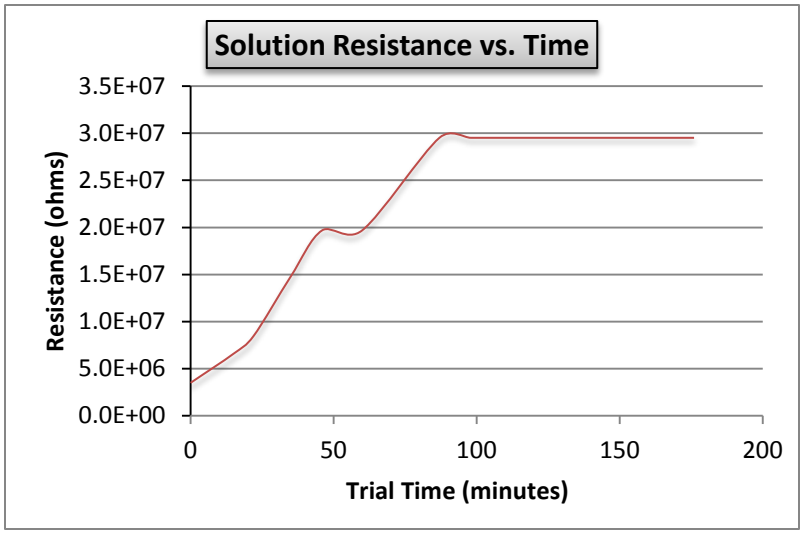

Figure 41: Trial 4 Solution Resistance versus Time Passed: The Solution resistance consistently increased until leveling off at rough 30 mega-ohms

from trial 4 were migration towards the cathode for another pH 9 solution, and the increased activity caused by increasing electrical potential and as a result current through the solution.

Trial 5

In trial 5 solution 4 was used in order to test the behavior of the protein without the interaction of the interfaces on the migration. Solution 4 was composed of the top phase of solution 2 with additional protein added to make observation easier. In previous experiments, it was observed that increased current would impart more rapid protein migration. As a result the power supply was operated at the rather high 2950 volts to ensure consistently high current. The primary goal of the experiment was to observe how the protein in the trial 1 top phases was interacting with the electrical field.

Date of Trial: February 28th, 2011
Solution: Solution 4
Apparatus: Large U-Tube
Power Supply: Bio-Rad 3000Xi

Maximum Potential	*3000 Volts*
Maximum Current	*5 mA*
Maximum Power	*35 W*
Constant Potential	*2950 Volts*
Anode Position	*left*

Initial Observations

Since only a single phase was used in this experiment the initial observations revealed that the solution was homogenous throughout. The color was generally light since the top phase of solution 2 is not the favored phase. Additionally some of the added protein did not fully dissolve into solution and appeared as small specks.

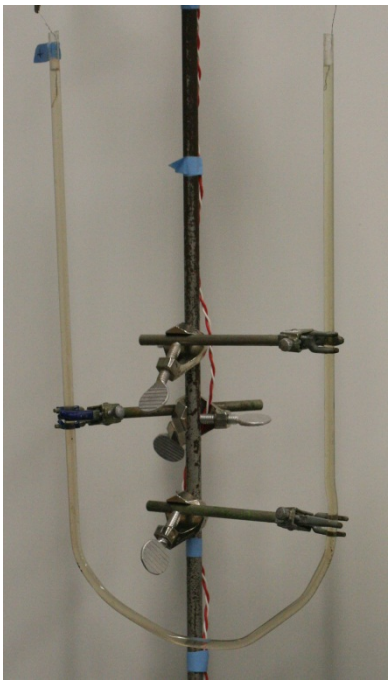

Figure 42 - Trial 4 Initial Observation: Homogenous throughout because of the lack of the PEG rich bottom phase

Observation 1 – 53 minutes

Unlike other trials there was a significant period of time between when the trial was initiated through the application of an electrical current and the first major observation. Prior to this point the only observable activity in the experiment was bubbling on anode and cathode. At the first observation point a region of darker solution, or a protein cloud, formed on the anode side of the bottom of the tube (Figure 43). This formation was similar to the dark migrating region in trial 4, since both formed in roughly the same area.

Figure 43 - Observation 1 Protein Cloud: Formation of a protein rich region in the anode side of the lower portion of the single phase

Observation 2– 66 minutes

Similar to the period between the initial and first observation, during the period between the first and second observation the anode and cathode electrodes continued to bubble. More pertinent was the migration of the protein cloud. As shown in Figure 44 the protein cloud migrated from its position in Figure 43 to a new position, roughly 3 centimeters closer towards the cathode. The direction of this migration was towards the cathode, the same direction as in trial 4. Additionally this first migration was very rapid and also corresponded with a darkening of the protein cloud.

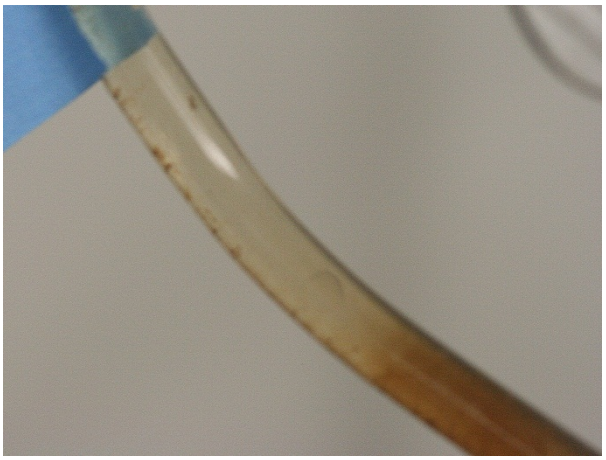

Figure 44 - Observation 2 Protein Cloud: Continued darkening of the protein cloud observed with rapid migration towards the cathode

Observation 3 – 77 minutes

Similarly to the period between the previous observational periods the period between the second and third observations had continued protein migration towards the cathode. As seen in Figure 45 the protein cloud has moved from the blue flag marking its position at the second observation further into the bottom of the U-Tube (~2cm). Additionally a change in the nature of the cloud was observed. Whereas previous observations noted a darkening of the cloud, corresponding with an increased protein concentration, the 3rd observation noted a different change. The protein cloud was no longer of a homogenous nature, instead it appeared particulated. This particulation of the protein was described as denaturation of the protein solution.

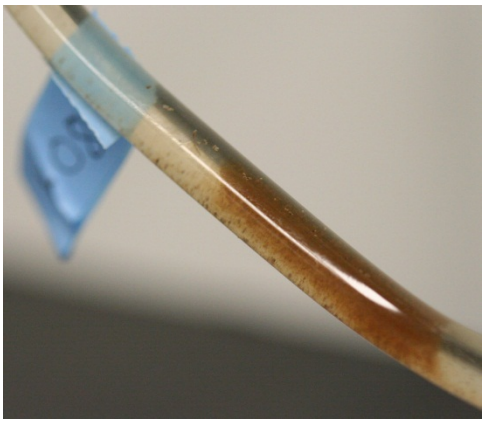

Figure 45 - Observation 3 Protein Cloud: Continued migration of the protein cloud in additional to apparent denaturation of the protein

Observation 4 – 104 minutes

For the 4th observation the primary focus was the protein cloud in the bottom of the U-Tube. The anode and cathode electrodes continued bubbling, but besides that there was no notable activity on either. The most striking change from the third observation was the continued denaturation of the protein in the protein cloud.

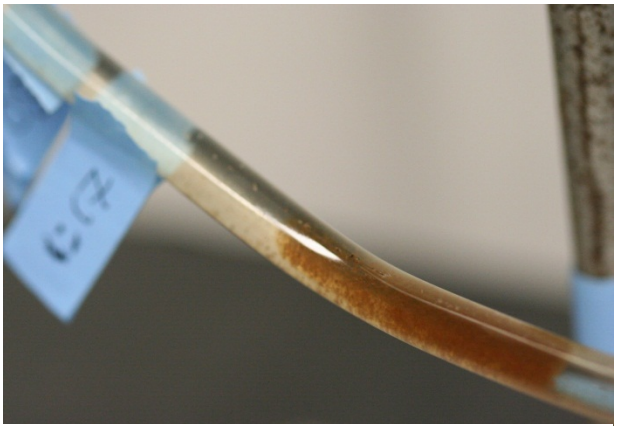

Figure 46 - Observation 6 Protein Cloud: Migration towards the cathode, though at apparently reduced rate; additionally extensive protein denaturation

From a distance the protein cloud appeared homogenous closer observation revealed the presence of small discreet collections of protein in the cloud (Figure 46). The protein cloud also continued its migration towards the cathode, though at a reduced rate.

Observation 5, 6 and 7 – 126 through 202 minutes

Since the behavior of the experiment in trials 5, 6 and 7 were so similar their observational periods were combined. As can be seen in figure 12 the protein continues to migrate towards the cathode though at ever decreasing rates. The blue tape markers in Figure 47 mark the location of the trailing edge of the protein cloud via the leading edge of the tape (or an arrow for the 6th observation, at 2:36). Clearly the distance between these markings got closer and closer as time passed corresponding with the decreasing rate of protein migration. While other observations noted increased particulation of the protein cloud these observations did not, it seemed the protein had particulated as much as it would. It seems that this decreased rate of migration corresponds strongly with the development of the denatured protein in the solution.

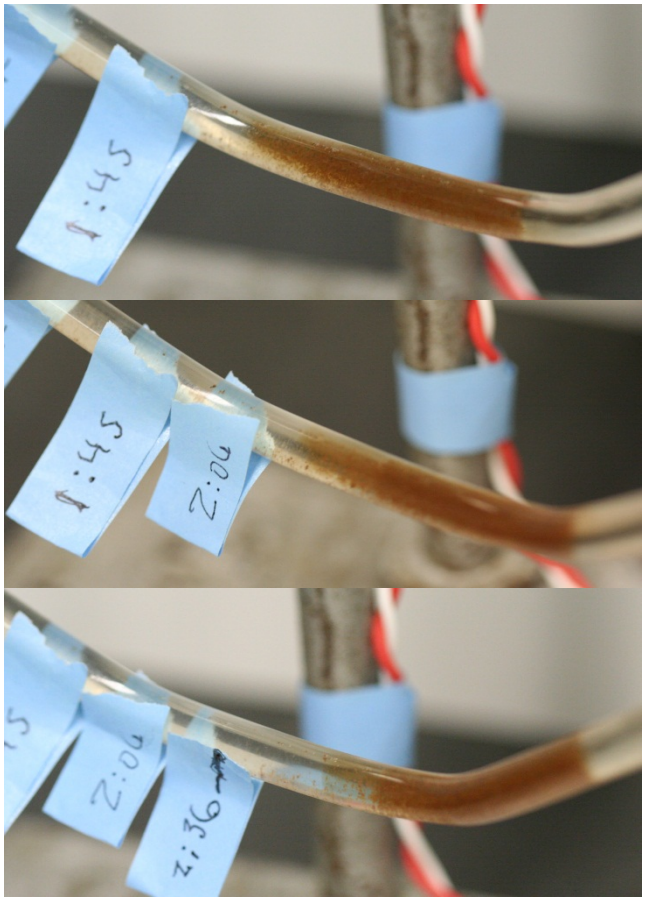

Figure 47 - Protein Migration in Observations 5,6 and 7: The protein cloud continues to migrate towards the cathode while exhibiting the heterogeneous denatured characteristics

Observation 8 – 262 minutes

The final observation in trial 5 noted similar behavior as previous observations. During the extended period between observation 7 and 8 the protein cloud migrated a small distance, though not

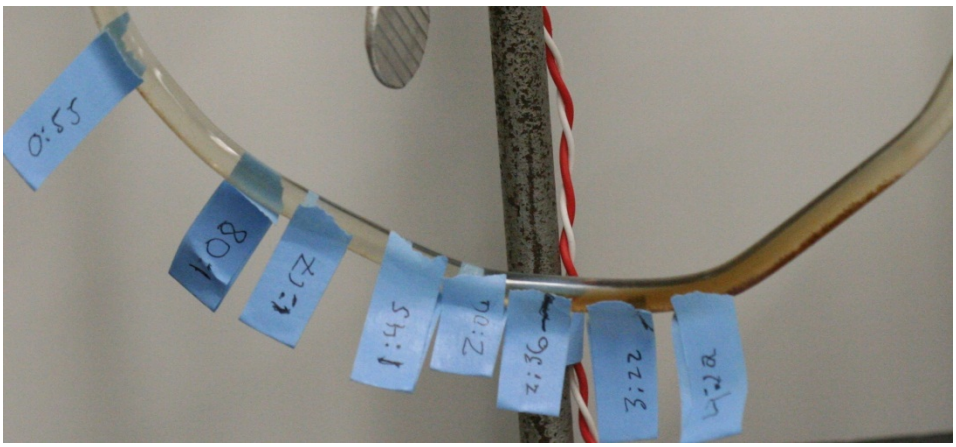

Figure 48 - Observation 8 Protein Cloud: Entire migration pattern of protein cloud is shown

nearly as far as other periods of times despite the long time between the observations. As shown in Figure 48 the migration pattern of the protein cloud was initially rapid, then continually slowed towards the bottom of the tube. Additionally it is possible to observe the continued denaturation of the protein in Figure 48 through the strongly particulated collection of protein on the bottom of the tube wall on the cathode side. The trial was halted because the protein cloud was no longer migrating; the final position was slightly up the bend in the U-Tube towards the cathode.

Summary of Observations

In trial 5 the primary observation was the migration of protein towards the cathode electrode. Initially forming on the anode side of the U-Tube close to the bottom of the tube, this cloud first concentrated then began migrating. The migration was initially very rapid, but corresponding to the observed denaturation of the protein it slowed as time passed. This denaturation was observed in other trials, but was particularly strong in trial 5. It was characterized by the particulation and de-homogenization of the protein cloud. Observation of the protein cloud noted that as it denatured the temperature of the glass tube immediately surrounding the protein cloud was warmer. Because of the correlation between denaturation of the protein and decreased and eventually halted protein migration, it was proposed that the particulation of the protein needed to be eliminated in order to induce more protein migration towards the cathode. Since heating of the solution was observed it was decided to attempt to control the solution temperature to counteract the decreased migration rate.

Trial 6

It was proposed that the protein denaturation observed in previous trials was a result of excessive heating of the protein in solution through resistance to the electrical current. To counter act this effect the small U-Tube was immersed in an ice bath (Figure 49). The intention was to limit solution heating by cooling the solution through the U-Tube wall. Solution 2 was selected because it would allow for a comparison to the results in trial 1.

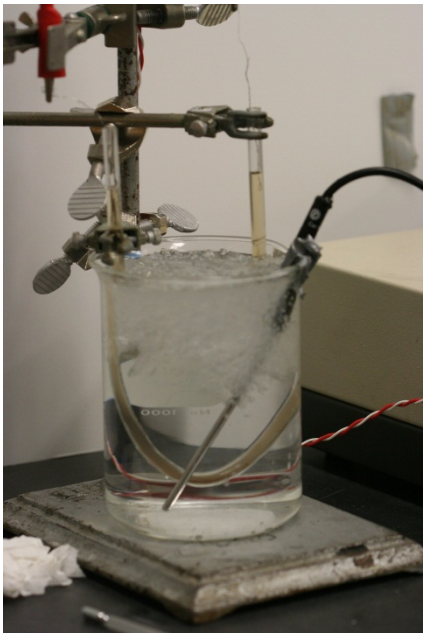

Figure 49 - Experimental Setup for Trial 6: Ice bath and small U-Tube with temperature probe

Date of Trial: March 8th, 2011
Solution: Solution 2
Apparatus: Small U-Tube in Ice Bath
Power Supply: Bio-Rad 3000Xi

Maximum Potential	*3000 Volts*
Maximum Current	*5 mA*
Maximum Power	*35 W*
Constant Current	*1 mA*
Later Reset To	
Maximum Potential	*3000 Volts*
Maximum Current	*5 mA*
Maximum Power	*35 W*
Constant Potential	*2950 Volts*
Anode Position	*left*

Initial Observations

Similarly to trial 1 which used solution 2 the interface was some want vaguely defined and definitely not as distinct as other solutions. This is shown in Figures 50 and 51, the anode and cathode interfaces respectively. In these figures the top and bottom phases are roughly the same color and the distinction is primarily from the viscosities of each phase. The initial temperature measurement was at 3.5 °C, and this remained the goal for the remainder of the experiment.

Figure 51 - Trial 6 Initial Observation of Cathode Interphase

Figure 50 - Trial 6 Initial Observation of Anode Interphase

Observation 1 – 12 minutes

At the first observation after the electrical field was applied to the solution evidence of protein migration was immediately

obvious. On the anode side a clear band began to form above the interface as the protein in the top phase began to migrate towards the cathode electrode through the interface (Figure 52). On the opposite side of the U-Tube by the cathode interface another characteristic trait of protein migration was observed. A dark band pictured in Figure 55 indicates the migration of protein towards the cathode electrode and possible migration inhibition at the interface.

Figure 52 - Observation 1 Anode Interphase: Formation of clear band beneath the interface as protein migrates towards the cathode

Figure 55 - Observation 1 Cathode Interface: Dark band formation due to inhibition of protein migration and establishment of new equilibrium

Observation 2– 27 minutes

At the second observation point the cathode interface continued to develop a dark band at the interface. The probable cause for the increased darkness at the interface is the continued migration of protein towards the cathode. As more protein moves towards this interface more and more of the protein gets inhibited causing an increased local concentration. The darker interface region on the cathode side is pictured in Figure 54. At the anode interface continued disruption was observed as the protein from the anode top phase migrated into the bottom phase towards the cathode electrode. A newer development was the formation of a protein cloud in the bottom phase of the U-Tube shown in Figure 53. At the 2nd observation point this cloud was diffuse, but previous experimental trials suggested that it would condense soon and become a point of interest. The temperature of the ice bath near the bend in the U-Tube (the temperature probe can be seen in Figure 53 as the bright steel rod in the picture foreground) was 0.8 °C.

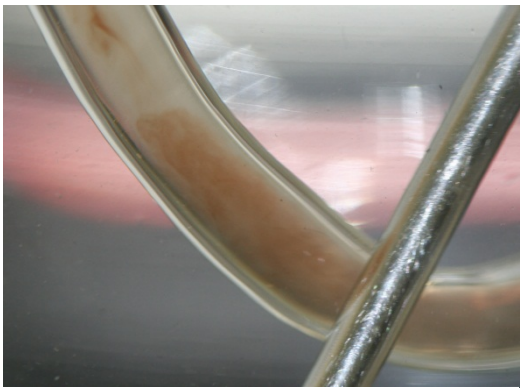

Figure 53 - Observation 2 Bottom Phase: Formation of a diffuse protein cloud in the bottom phase

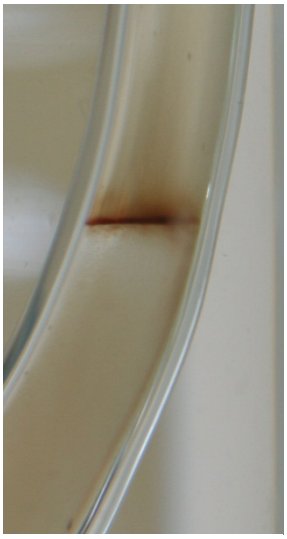

Figure 54 - Observation 2 Cathode Interface: Dark band at interface has grown more intense

Observation 3 – 47 minutes

At the third observation point the clear band above the anode interface continued to grow, indicating continued migration of protein out of the top phase (Figure 58). On the cathode side the interface still remains dark, but has begun to diffuse towards the cathode electrode. This diffusion is clear in Figure 58 where a clear band has formed over the interface after a region of higher protein concentration and

before another region of high concentration. The diffusion of protein through the interface supports observations from other trials where the interface provided limited inhibition of protein migration. The final region of observation was the bottom phase where the protein cloud concentrated and began to migrate towards the cathode. The migration of this cloud was rather rapid and the new positioning can be seen in Figure 56. The temperature at this observation was 1.9 °C.

Figure 58 - Observation 3 Anode Interface: Clear band above interface continues to grow

Figure 57 - Observation 3 Protein Accumulation: Protein cloud condensed and began to migrate towards the cathode

Figure 56 - Observation 3 Cathode Interface: Dark band at interface remains, heavy diffusion through interface into top phase

Observation 4 – 54 minutes

At the 4th observation point the primary change observed was continued migration of the protein cloud in the bottom phase. By comparing Figure 59 to Figure 57 it is possible to notice how the leading edge of the protein cloud has moved (a small burn mark on the outside of the tube is present in both pictures for a reference). Temperature at this time was 1.3 °C.

Figure 59 - Observation 4 Protein Accumulation: Cloud continues to migrate towards cathode

Observation 5 – 89 minutes

After a significant period time a 5th observation was made on the tube. Anode interface behavior is similar as previous observations, while cathode interface remains roughly the same as it was at the third observation. A thin dark band and diffuse region above the interface is not remarkably different (Figure 60). Similarly to previous observations the protein accumulation in the bottom phase has

Figure 60 - Observation 5 Cathode Interface: Dark band is still present at the interface with a diffuse region above and clear region below

continued to migrate towards the cathode electrode. While the protein cloud did continue to move the rate at which it was moving was vastly decreased from other observation periods. Again it is possible to observe the relative migration velocity via the presence of the burn mark on the tube (Figure 61).

Figure 61 - Observation 5 Protein Accumulation: Continued, yet slowed migration of protein towards the cathode

Observation 6– 114 minutes

The final observation, observation 6, did not reveal any significant change in the experiment suggesting steady state had been reached. A final picture of the entire bottom phase, shown in Figure 62, shows the final resting spot for the protein accumulation. Also observable in Figure 62 is the cathode interface which still exhibits the dark band at the interface and diffuse region above.

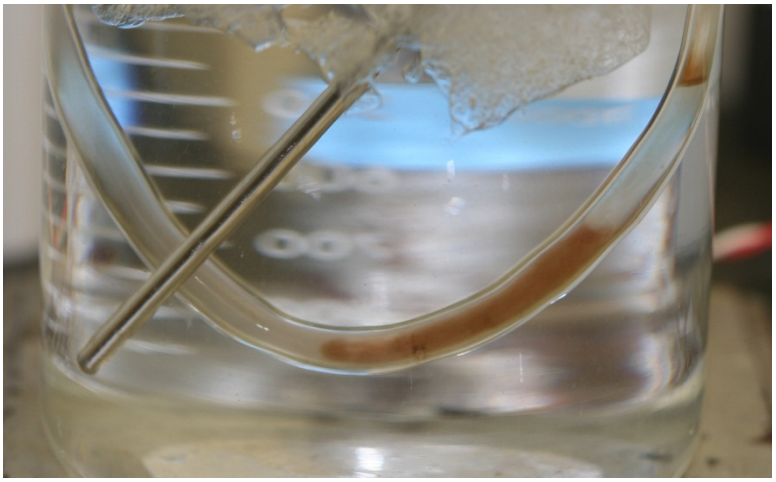

Figure 62 - Observation 6 Bottom Phase: Protein accumulation and cathode interface

Summary of Observations

The primary purpose of trial 6 was to attempt to limit protein denaturation through external temperature regulation via an ice bath. This attempt was generally successful as very little precipitation of protein was observed. By limiting protein denaturation it was possible to observe the difference in behavior between the normal and denatured protein. Typical of previous experiments the protein migrated towards the cathode electrode before stopping as it attempted to move up the cathode leg. Possibly this halt to protein migration is a result of the increasing electrical resistance of the solution as ions are depleted by carrying the electrical current. Also of importance was the limited effect of the interface on protein migration. While a localized region of higher concentration formed at the cathode interface, the protein simply diffused through this region.

Trial 7

Trial 7 was the first trial to use the higher pH solution, solution 5. This solution was formulated to work around the issue of ion depletion in the previous trials. An observed increase in resistance in the previous trials (via a correlation between the decreasing current at constant potentials and Ohm's Law V=I*R) was theorized to be a depletion of the ions in the solution between the electrodes. The proposed mechanism for this depletion was a migration of the ions similar to that of the protein; the applied electrical field would induce a migration of positively and negatively charged ions towards the oppositely charged electrode. Ion depletion became an issue because the increased solution resistance was more than the power supply could overcome in order to provide a consistent 1mA of current. Additionally the increased solution resistance caused a vast increase in solution heating, as explained by Joule's Law; $P=V^2/R$, where P equals the power dissipated by a resistor (the solution in this case), V is potential difference between the electrodes and R is the resistance of the solution. As the power supply worked to maintain current by increasing potential and as the solution resistance increased as ions moved towards each electrode, the power dissipated by the solution would still increase. This power would be absorbed as heat in the solution, which was a proposed cause for the observed protein denaturation.

Additionally, because the current through the solution is the driving force for protein migration, a decrease in current would most likely cause an equivalent decrease in migration. This would agree with the observations of rapid initial migration followed by progressively slower migration as time passed. A higher pH solution was selected in order to provide a greater initial concentration of ions to carry the current. The small U-tube was selected because the shorter distance between the electrodes would decrease overall resistance between the electrodes.

Date of Trial: March 19th, 2011
Solution: Solution 5
Apparatus: Small U-Tube
Power Supply: Bio-Rad 3000Xi

Maximum Potential	*3000 Volts*
Maximum Current	*5 mA*
Maximum Power	*35 W*
Constant Current	*1 mA*
Later Reset To	
Maximum Potential	*3000 Volts*
Maximum Current	*5 mA*
Maximum Power	*35 W*
Constant Potential	*2998 Volts*
Anode Position	*left side in all pictures*

Figure 63 - Initial Observation of Entire U-Tube for Trial 7

Initial Observations

Since solution 5 used a different buffer composition (pH 11) than previous

trials the phases appeared reversed with the top phase being darker than the bottom phase. Because of the great difference in color between the top and bottom phases the color difference is very obvious, making the interface very well defined. The bottom phase initially appeared completely clear.

Observation 1 – 6 minutes

Immediately after starting the electrical current through the tube protein began to precipitate on the platinum wire of the anode electrode (white formation in Figure 65). While the mechanism for this precipitation was not investigated this process showed very clearly the trend for protein migration towards the anode. Further down the tube at the anode side interface an immediate disruptance of the interface was observed. The area above the interface began to clear out as the protein from the top phase moved rapidly towards the electrode (Figure 64). This apparent migration continued, and was observed via the increased size of the clear area above the interface.

Figure 65 - Observation 1 Anode: Protein precipitation

Figure 64 - Observation 1 Anode Interface: Protein migration away from interface towards electrode

Corresponding to the migration of protein in the anode side top phase towards the anode electrode the protein in the cathode side top phase was observed migrating towards the bottom phase. This falls in line with the migration on the anode side because the direction of protein movement is the same; away from the cathode towards the anode. Of particular interest is the nature of the cathode interface. Immediately above the interface it is the homogenous top phase, but at and below it is far from homogenous. At the interface a dark band has formed (Figure 66), potentially showing a region of protein migration inhibition; the buildup of protein as it is held back from moving towards the anode would be a darker band. Below the interface a somewhat homogenous region of darker solution (higher protein concentration) followed by a region where there are observable currents of high protein concentration moving away from the interface.

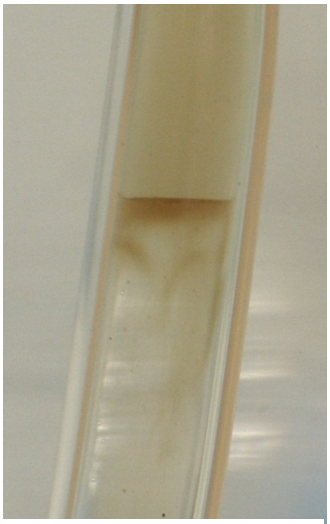

Figure 66 - Observation 1 Cathode Interface: Diffuse dark band below interface formed as protein migrates through interface

Observation 2– 24 minutes

At the second observation point similar behavior continued. More protein precipitated on the anode electrode; at this point the protein collection was becoming rather large and would at certain points in time release from the electrode wire. The

released protein collected at the top of the solution (Figure 67). Below the anode electrode tip at the anode side interface the protein continued to collect and migrate towards the anode electrode. As seen in Figure 68 the protein has pushed towards the outer wall of the tube and has concentrated since the last observation. Under the interface in the bottom phase a diffuse cloud of protein was observed moving towards the interface. Since there is no dark band at the interface it appears as though the interface is in no way inhibiting the migration of protein towards the anode. On the cathode side protein continues to migrate through the interface. The dark band between the top and bottom phase has lightened, suggesting that concentration in the top phase of the cathode leg is decreasing (Figure 69). The protein appears to reach the interface as a homogenous cloud, but then diffuses into currents after moving through the interface.

Figure 68 - Observation 2 Anode Interphase: Migration of protein through and away from interface towards anode electrode

Figure 67 - Observation 2 Anode Electrode: Small white formation of protein precipitate on the electrode tip, larger formation of released protein at the surface of the top phase

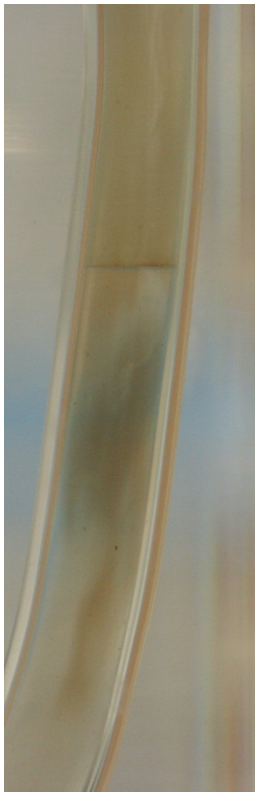

Figure 69 - Observation 2 Cathode Interphase: Protein continues to diffuse through interface boundary

Observation 3 – 41 minutes

At the third observation point there was very limited change from the second observation. Protein continued to precipitate on the anode and protein continued to migrate out of the top phase on the cathode side into the bottom phase through the interface. One area of particular interest was the interface in the anode leg. Previous observations had made note of the decreasing color in the bottom phase. At this point the bottom phase has become almost entirely clear (Figure 70), while the region immediately above the interface is very dark with high protein concentration.

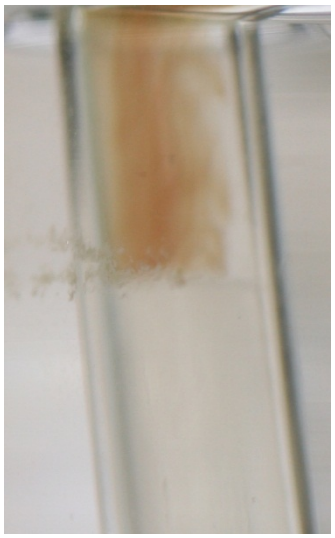

Figure 70 - Observation 2 Anode Interphase: Bottom phase has become completely clear; protein cloud in top phase begins at the edge of the interface

Observation 4 – 54 minutes

The period of time between the 3rd and 4th observation had very limited changes. There continued to be protein formation on the anode electrode, with periodical releases of the precipitate. At the

cathode interface both phases had completely cleared out as the protein moved into the bottom phase towards the anode. The anode interface appeared similar to the 3rd observation, just with less protein. It appears as though the protein crossed the interface en masse and then began to slowly migrate towards the electrode (Figure 71).

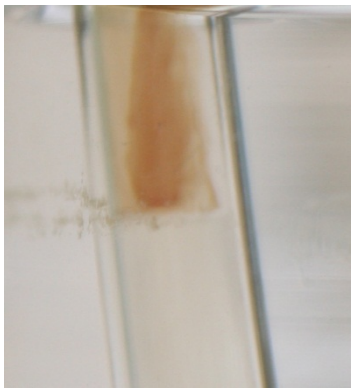

Figure 71 - Observation 4 Anode Interface: Decreasing protein concentration above interface as protein migrates towards electrode

Observation 5 – 63 minutes

By the 5th observation very little had changed. The cathode interface was very poorly defined as the protein in both phases on this side of the U-Tube had been depleted as the protein migrated towards the anode electrode. Similarly the bottom phase had been depleted of protein causing it to appear clear. At the anode interface there was very little change from the 4th observation; a buildup of protein immediately above the interface remained in place but had begun to clear up as more of the protein moved towards the electrode. The remaining observations at *1:16, 1:24* and *1:36* exhibited the same behavior with very limited changes. Following the 8th observation it was decided to halt the experiment because it had apparently reached steady state.

Summary of Observations

The most important observation in trial 7 was the lack of protein denaturation. In previous experiments the formation of solidified protein in solution (not the white precipitate observed on the electrodes, but rather dark non-buoyant particles) marked the denaturation of the protein. This was achieved by using a stronger buffer solution to provide a greater initial concentration of ions to carry the electrical current (Figure 72 illustrates how resistance of the solution remains under 1.4 mega-ohm). As predicted this worked effectively to limit protein denaturation. By eliminating the protein denaturation effect it was possible to carry out the trial to apparent completion. Throughout the experiment the protein migrated towards the anode, through both interfaces with limited inhibition. The protein migration continued until the cathode side top phase had become fully depleted of protein, followed by the bottom phase becoming depleted of protein.

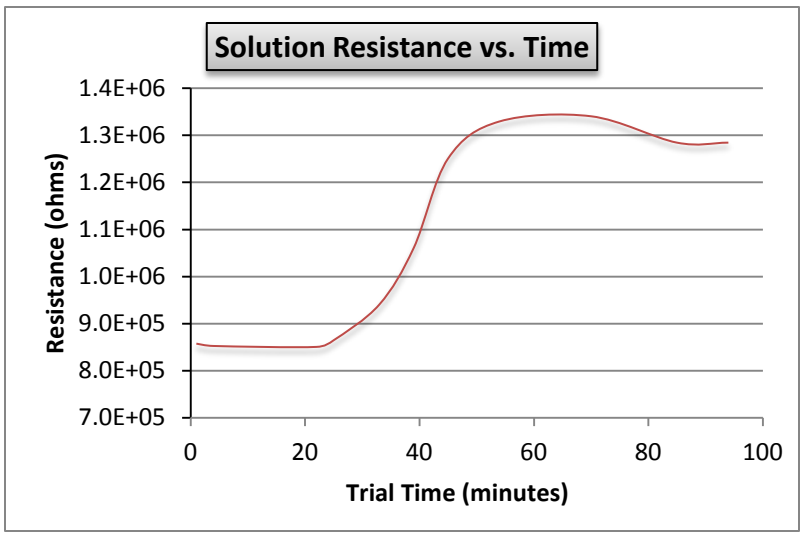

Figure 72: Trial 7 Solution Resistance

Trial 8

The purpose of trial 8 was to test the effect of the applied electric field on the top phase of the pH 11 solution (solution 5). The higher pH solution was used to attempt to counteract the ion depletion effect observed during trials using the pH 9 solutions by providing a greater concentration of ions. Additionally the top phase of the solution was selected in order to eliminate any effect of the interface on protein migration. The observed protein migration in this trial would provide a strong comparison to the results of trial 7 because both trials used the same solutions (albeit trial 8 only used the top phase), but trial 8 would not have any effect from an interface.

Date of Trial: March 26th, 2011
Solution: Solution 5 – Top Phase
Apparatus: Straight Tube
Power Supply: Bio-Rad 3000Xi

Maximum Potential	*3000 Volts*
Maximum Current	*5 mA*
Maximum Power	*35 W*
Constant Current	*1 mA*
Anode Position	*left*

Initial Observations

Since only the top phase of solution 5 was used there is no interface to observe. At the initial observation, prior to the application of the electrical field, there is an even color distribution corresponding to the homogenous nature of the single phase (shown in Figure 73). The color is not exceptionally dark, rather somewhere in the middle of the spectrum.

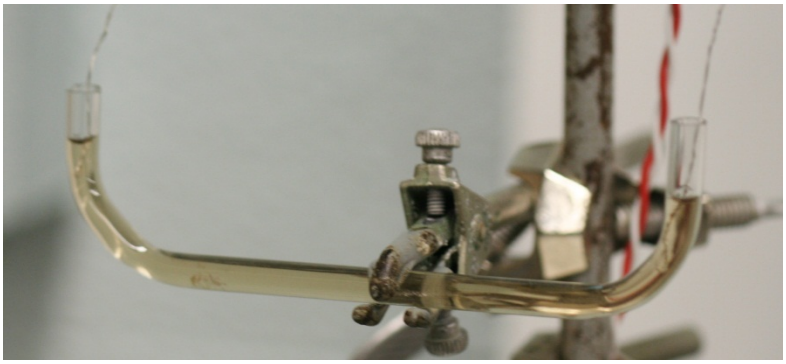

Figure 73- Initial Observation of Straight Tube for Trial 8: Even distribution of color through the tube

Observation 1 – 8 minutes

At the first observation point the standard observation procedure was modified to match the varied experimental setup. Since there was no interface to observe in this trial the observations were focused on the tip of the anode electrode, the region in the center of the straight tube and the tip of the cathode electrode. The typical fizzing was observed on the cathode wire, corresponding to the electrolysis of

water (Figure 74). Similar to trial 7 there was an immediate buildup of protein on the tip of the anode wire, as shown in Figure 75. At this point in time the potential was recorded at 340 volts and the current was remaining constant at 1mA.

Figure 74 - Observation 1 Cathode: Fizzing on electrode

Figure 75 - Observation 1 Anode: Protein accumulation observed as small white solid on electrode

Observation 2– 16 minutes

As time passed from the first observation point more protein developed on the anode electrode wire until roughly 15 minutes into the trial when the protein buildup released from the wire and collected in the bubbles at the solution-atmosphere surface. The cathode exhibited continued fizzing of no real interest. At this point in time the beginnings of a protein cloud were observed left of the center (on the anode side). Corresponding with this increased concentration near the anode a color gradient was observed from the anode to cathode, with the color getting lighter towards the cathode (Figure 77). Potential was measured at 400 volts; this was the peak voltage for the experiment, but was not drastically higher than the initial measured potential difference indicating the reduced solution resistance.

Figure 77: Observation 2 Full Tube: Color gradient darkening from cathode to anode, protein accumulation near the bend towards the anode electrode

Figure 76: Observation 3 Full Tube: Color gradient even more obvious than previous observation

Observation 3 – 26 minutes

During the time period between

the 2nd and 3rd observations the solution exhibited familiar behavior. The cathode continued to bubble on the wire with no other developments of interest, and the anode electrode continued the cycle of protein generation and release. While the electrodes did not provide any intriguing changes the area in between did. The solution in the middle of the tube continues to collect and migrate towards the anode. The accumulation of protein is primarily directed towards the bottom of the tube and appears 'swept back' towards the anode as it moves towards the top of the tube (Figure 76). Additionally the color gradient within the tube appears less gradual with a sharp transition from light to dark roughly in line with the dark concentration in the center of the tube (Figure 78). At this observation point it appeared that the protein around the cathode electrode had completely migrated away with the solution near the electrode essentially clear.

Figure 78 – Close-up of Protein Accumulation: Swept back nature exhibits the migration direction for protein

Observation 4 – 31 minutes

Similarly to the period of time between the 2nd and 3rd observations, the time period between the 3rd and 4th observations continued with familiar behavior. Both the cathode and anode continued with their trial typical activity, fizzing and protein buildup and release respectively. Again the interest was the area between the electrodes. The color gradient (corresponding to the protein concentration gradient) continued to become more distinct, with the concentrated parts of the solution becoming very dark and the concentrated parts becoming very clear (Figure 80). The very dark concentration in the middle of the tube continued to darken, though it exhibited no apparent movement (Figure 79). This observed lack of migration is contrary to the general trend for protein migration towards

Figure 80: Observation 4 Full Tube: Very distinct color difference between protein rich and protein poor regions

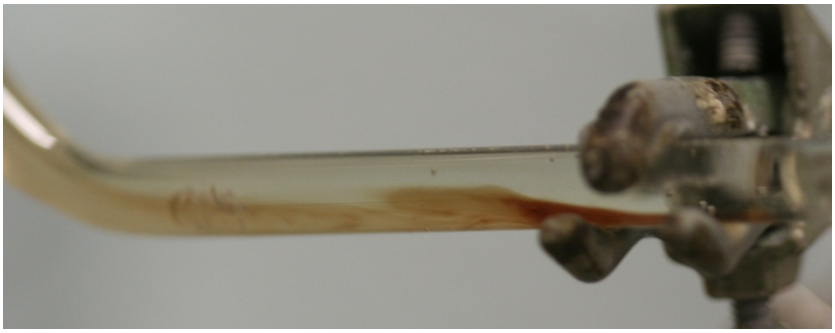

Figure 79 – Close-up of Protein Accumulation: The area of high protein concentration in the center of the tube appears to have become more concentrated but has not migrated at all

the anode.

Observation 5 – 39 minutes

At the 5th observation point the familiar trend of fizzing at the cathode and protein accumulation on the anode was noted. The middle region of the tube also exhibited similar behavior as previous observations. The concentrated area in the center of the tube still appears stagnant, with a swept back profile (Figure 81). Essentially the solution appeared unchanged from the previous observation.

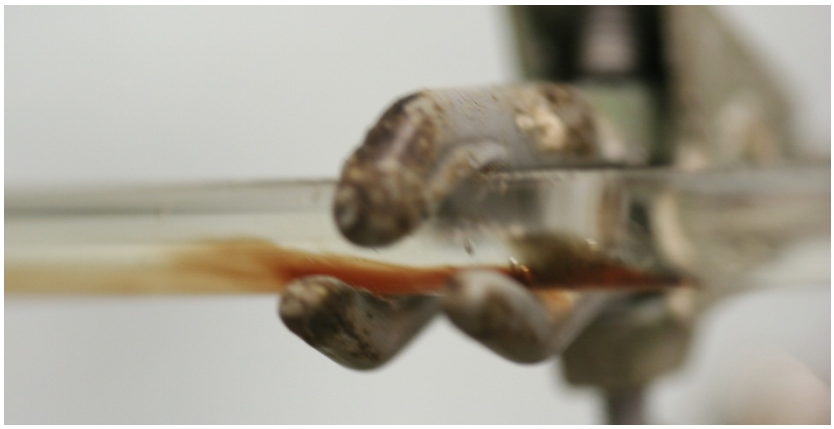

Figure 81 - Observation 5 Protein Accumulation - Close-up of stagnant concentrated region in the middle of the tube

Observation 6 – 52 minutes

By the 6th observation it experiment has seemed to reach a non-active state. Both electrodes exhibited the same behavior as other observations, and the region in the middle of the tube still contained the stagnant protein accumulation. Of particular interest during this observation was the profile of the protein rich and protein poor parts of the solution. In previous observations the 'swept back' nature of this profile was noted, but as is seen in Figure 83. Potential was measured at 377 volts at this observation point, indicating roughly equivalent resistance to other observation points.

Figure 83 - Observation 6 Protein Accumulation: The dark area continues to be stagnant

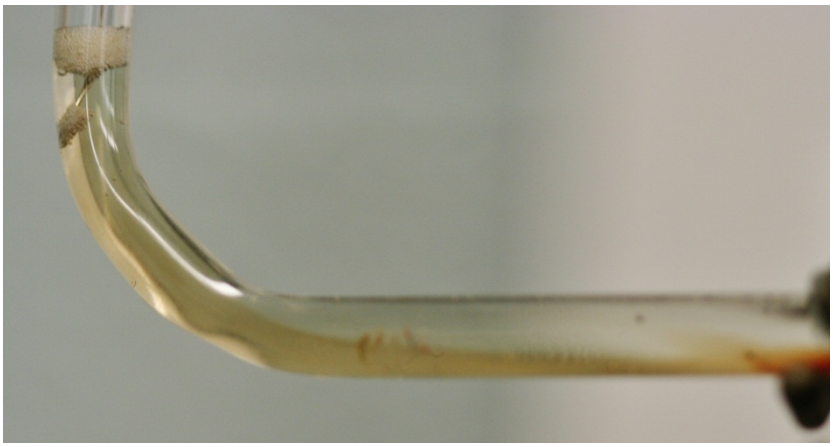

Figure 82: Swept-back Profile of High Relative Protein Concentration

Observation 7 – 63 minutes

Similar to the 6th observation point, the 7th observation did not

exhibit any significant change. It was determined that the experiment had reached steady state and would not experience any further changes by continuing.

Summary of Observations

Trial 8 was devised in order to observe the effect of an applied electric field on a single phase solution. By eliminating the interface a comparison to trial 7 could be used to examine any differences in observed protein migration without the interface to potentially inhibit migration. Throughout the trial protein collected on the anode electrode as a white, buoyant precipitate. Conversely on the cathode electrode there was no protein precipitation. This falls in line with the observation of protein migrating towards the anode and away from the cathode. The most intriguing changes occurred in the middle region of the tube where the solution sharply partitioned into protein rich and protein poor regions. Initially this portioning appeared to be simple concentrating of protein in the migration process, but as time passed the region directly in the middle did not migrate. Instead it continued to concentrate and remained stagnant. Despite the different behavior in the middle, a general trend of protein migration towards the anode was observed, similar to the migration in trial 7. The rate of migration between the trials was not significantly different, suggesting the interface has a limited migration inhibition effect at partition coefficients close to 1.0.

Conclusions

The easy conclusion to reach from the experimental results is that using a two phase solution with a pH of 9 will not allow the determination of whether or not the protein is stopped at the phase barrier from the preferred phase into the non-preferred phase. The protein being hold up at the phase barrier cannot be examined using the pH 9 system we used because the protein forms a cloud of denatured particles in the bottom phase and stops moving. It is hypothesized that this occurs because the buffer ions are carried through the solution to one leg of the system vastly lowering the conductivity of the solution. The lower conductivity results in a higher resistance for the solution. The increased resistance of the solution results in resistive heating that is believed to be the cause of the protein denaturing. The denatured protein forms a cloud that settles in the bottom of the u-tube. A pH 9 solution that had a higher initial concentration of buffer ions could have worked for the purpose of these experiments.

The two phase solution with a pH of 11 allows for the examination of protein crossing from the non-preferred to the preferred phase since the protein moves from the cathode leg all the way to the anode leg. The interfaces exhibit limited protein migration inhibition.

The apparent inhibition of the protein migration at the interfaces is a result of the establishment of a local equilibrium. The protein moving from one side of the interface to the other side raises the concentration on the side that the protein migrated to. The concentration on the side of the interface that the protein migrated from increases as well to maintain the local equilibrium. This gathering of protein can be seen as the dark rim that forms on the interface. Throughout the balancing of concentrations protein continues to move through the interface and move towards the anode. The interface clears up as enough protein is moved through the interface to lower the concentrations of both sides of the local equilibrium.

Recommendations

The majority of recommendations have to do with changing the experimental apparatus to improve the results of the experiments. The first change that is recommended for the apparatus is to use a u-tube with an internal diameter that is larger than the 5mm of the original u-tubes. The increase in diameter would help the flow of current through the system as well as help decrease the effects of the viscosity of solutions. The length between the electrodes should also be decreased so that the required potential voltage is not as high. Also it is recommended that a power supply capable of supplying more than 3000 volts used. The problem of current degradation that was experienced in the runs with the pH 9 solution might have been partially counteracted by an increased potential current.

It was noticed throughout the experiments that where the protein cloud had formed the u-tube would be warm to the touch. It might be possible to control this heating with a controlled environment held at three to four degrees Celsius. An effective method of controlling the environment would have to be created because an ice bath was inefficient. Also the problem of depleted buffer ions could be overcome if an apparatus that was capable of circulating buffer ions was developed for the experiments to be run in.

It is suggested that solutions of varying pH be tested because a wider range of values should be tested to determine the effects of the pH on the experiment. Perhaps additional test at pH 1, 3, 5, 7, and 13 could be run to allow for a more complete picture of protein migration in various two-phase systems. Also a pH 9 solution with a higher initial buffer ion concentration should be tested since it might solve the problem of buffer ion depletion. The two phase solutions should also be tested with partition coefficients further away from one because this will give a more visible migration since the original concentration of protein in each phase wouldn't be as close.

Works Cited

Bio-Rad Laboratories. (n.d.). *Bio-Rad Model 3000xi Computer Controlled Power Supply: Instruction Manual.* Retrieved March 2011, from Bio-Rad: http://www.bio-rad.com/webroot/web/pdf/lsr/literature/Bulletin_9019.pdf

Chaplin, M. (2004, December 20). *Aqueous biphasic systems.* Retrieved March 24, 2011, from London South Bank University: http://www.lsbu.ac.uk/biology/enztech/biphasic1.html

Clark, W., & Lindblad, M. (2011). Numerical Analysis of Two-Phase Electrophoresis. *Seperation Science and Technology*, (Accepted for Publication).

Clark, W., & Marando, M. (1993). Two-Phase Electrophoresis of Proteins. *Seperation Science and Technology, 28.8*, 1561-1577.

Cuatrecasas, P. (1970). Protein Purification by Affinity Chromatography. *The Journal of Biological Chemistry*, 3059-3065.

Cummins, P. M., & O'Connor, B. F. (2011). Hydrophobic Interaction Chromatography. *Methods in Molecular Biology, 681*, 431-437.

Levine, M. L., & Bier, M. (1990). Electrophoretic Transport of Solutes in Aqueous Two-phase Systems. *Electrophoresis, 11*, 605-611.

Smolders, C., Aartsen, J., & Steenbergen, A. (1971). *Liquid-liquid Phase Seperation in Concentrated Solutions of Non-crystallizable Polymers Polymers by Spinodal Decomposition.* Retrieved March 24, 2011, from Ekaya Solutions: http://www.ekayasolutions.com/Research/LiteratureGuide/DryingThinFilms/SmoldersSpinodalDecom_71.pdf

Appendix: COMSOL Model Report

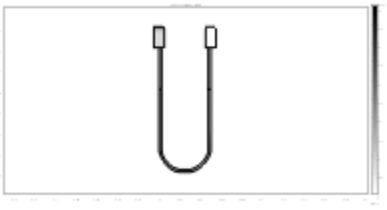

1. Table of Contents

2. Model Properties

Property	Value
Model name	
Author	
Company	
Department	
Reference	
URL	
Saved date	Mar 17, 2011 3:58:36 PM
Creation date	Aug 13, 2010 11:26:35 AM
COMSOL version	COMSOL 3.5.0.603

File name: R:\MQP\Levine-3.mph

Application modes and modules used in this model:

- Geom1 (2D)
  - Electrokinetic Flow (Chemical Engineering Module)
  - Electrokinetic Flow (Chemical Engineering Module)
  - Conductive Media DC (AC/DC Module)

3. Constants

Name	Expression	Value	Description
cond	0.04	0.04	
V0	200	200	
R	8.314	8.314	
T	298	298	
D	6.8e-11	6.8e-11	
Dt	D	6.8e-11	
Db	D*0.34	2.312e-11	
cb0	0.2	0.2	
ct0	0.008	0.008	
M	10000	10000	
K	1	1	
char	-20	-20	
mut	Dt/(R*T)	2.744623e-14	
mub	Db/(R*T)	9.331717e-15	

4. Geometry

Number of geometries: 1

4.1. Geom1

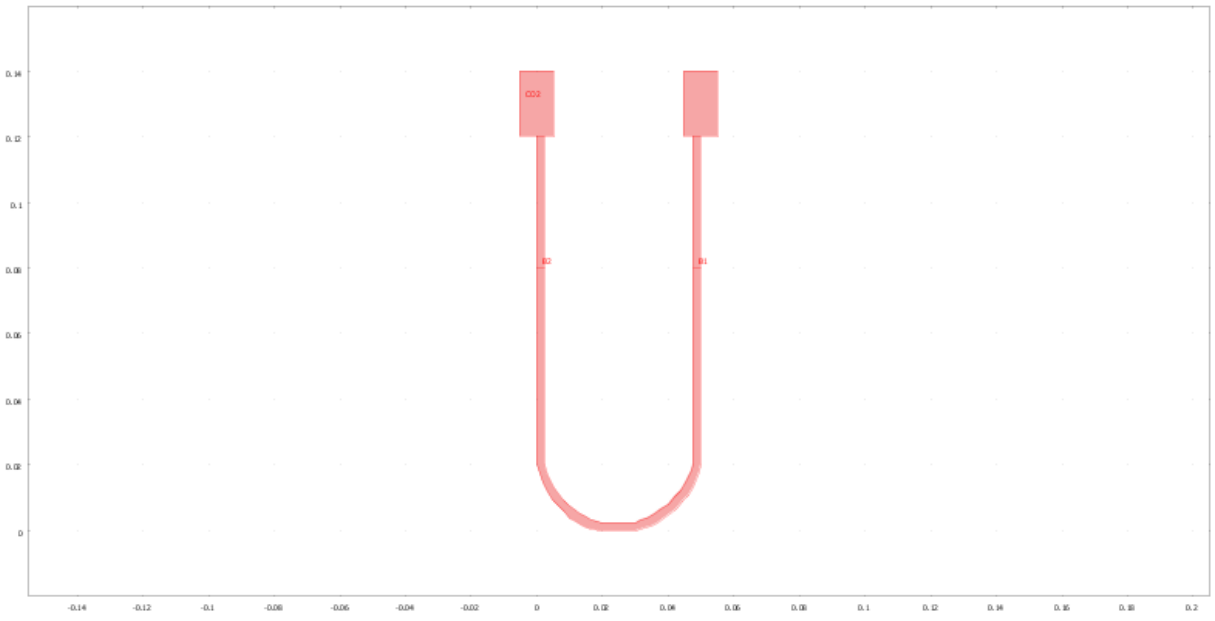

4.1.1. Point mode

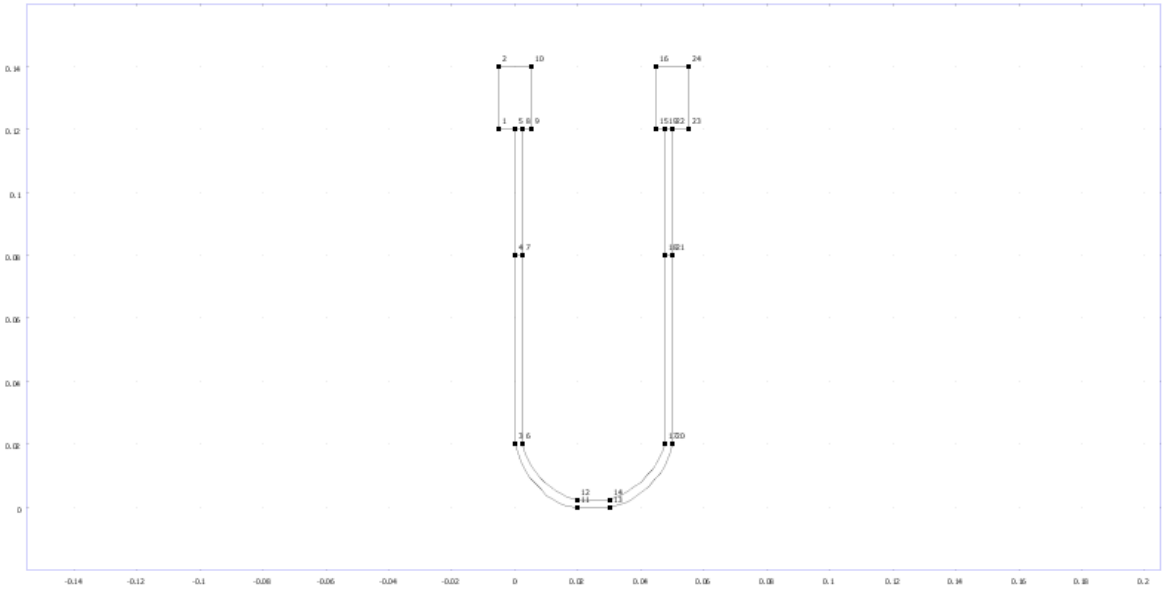

4.1.2. Boundary mode

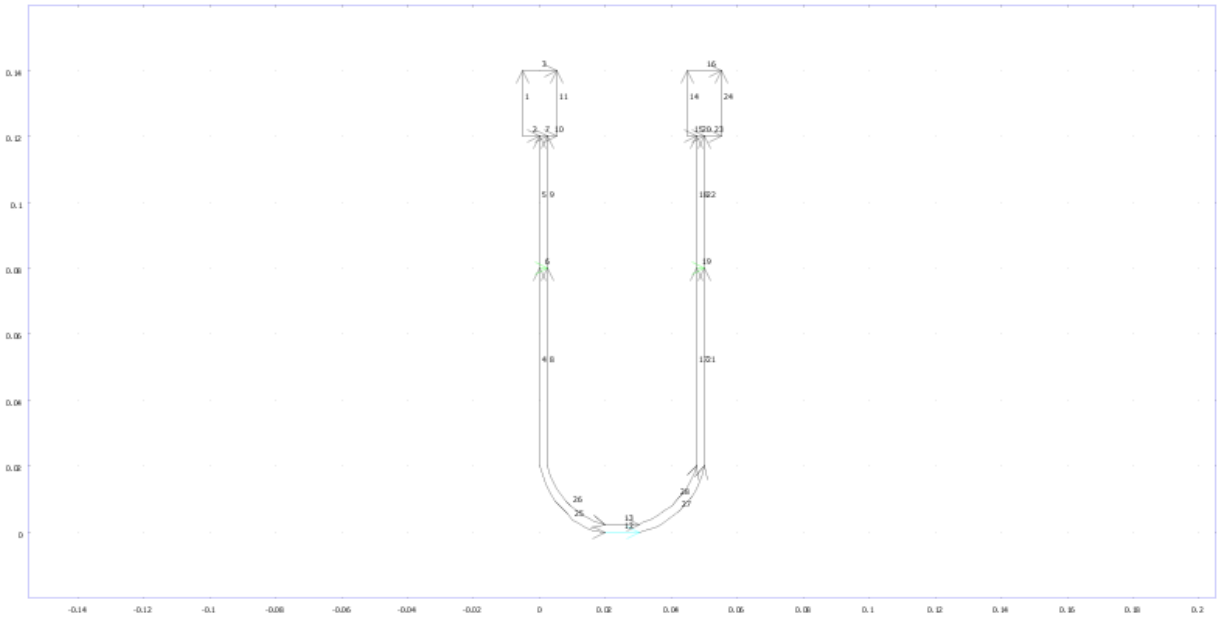

4.1.3. Subdomain mode

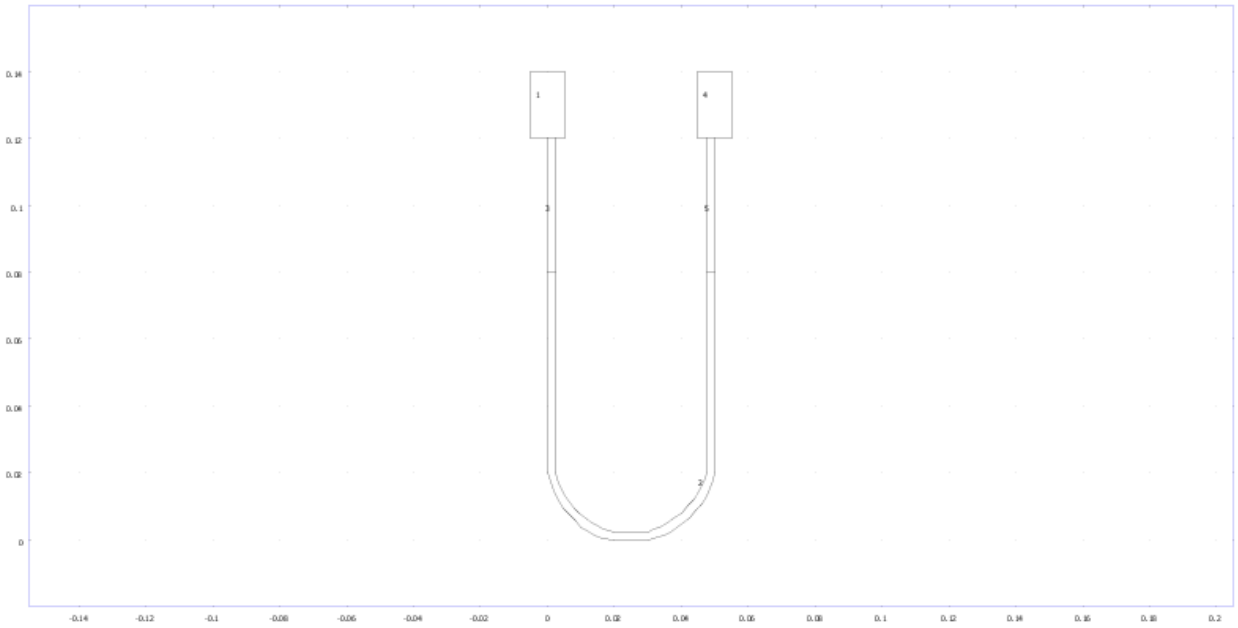

5. Geom1

Space dimensions: 2D

Independent variables: x, y, z

5.1. Expressions

5.1.1. Subdomain Expressions

Subdomain		1, 3, 5	2	4
c_all	mol/m^3	ct	cb	ct

5.2. Mesh

5.2.1. Mesh Statistics

Number of degrees of freedom	217030
Number of mesh points	27299
Number of elements	53657
Triangular	53657
Quadrilateral	0
Number of boundary elements	1207
Number of vertex elements	24
Minimum element quality	0.705
Element area ratio	0

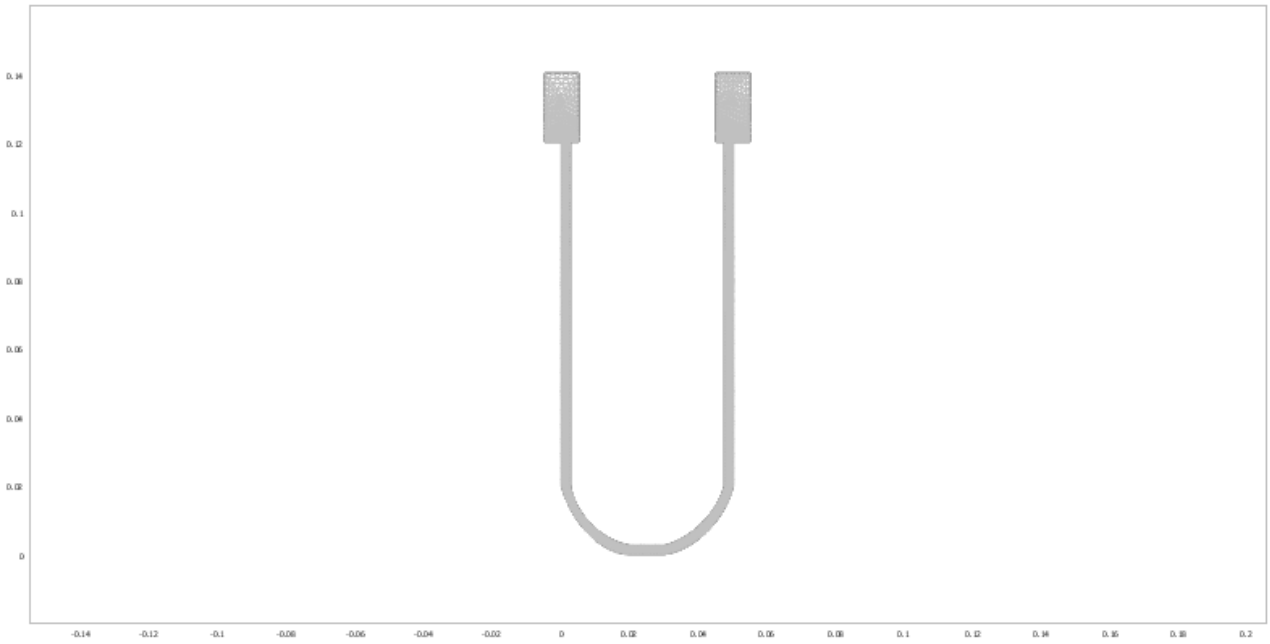

5.3. Application Mode: Electrokinetic Flow (chekf)

Application mode type: Electrokinetic Flow (Chemical Engineering Module)

Application mode name: chekf

5.3.1. Scalar Variables

Name	Variable	Value	Unit	Description
F	F_chekf	96485.3415	s*A/mol	Faraday's constant

5.3.2. Application Mode Properties

Property	**Value**
Default element type	Lagrange - Quadratic
Analysis type	Transient
Equation form	Non-conservative
Equilibrium assumption	Off
Frame	Frame (ref)
Weak constraints	Off
Constraint type	Ideal

5.3.3. Variables

Dependent variables: ct

Shape functions: shlag(2,'ct')

Interior boundaries not active

5.3.4. Boundary Settings

Boundary		1-3, 5, 9-11, 14-16, 18, 22-24	6, 19
Type		Insulation/Symmetry	Flux
Inward flux (N)	mol/(m^2·s)	0	**M*(K*cb-ct)**

5.3.5. Subdomain Settings

Subdomain		1, 3, 5	4
Diffusion coefficient (D)	m^2/s	**Dt**	**Dt*1000**
Mobility (um)	s·mol/kg	**Dt/(R*T)**	**Dt/(R*T)**
Charge number (z)	1	**char**	**char**
Potential (V)	V	**V**	**V**
Isotropic diffusion switch (idon)		**1**	**1**
Streamline diffusion switch (sdon)		**1**	**1**

Subdomain initial value		1, 3, 5	4
Concentration, ct (ct)	mol/m^3	ct0	ct0

5.4. Application Mode: Electrokinetic Flow (chekf2)

Application mode type: Electrokinetic Flow (Chemical Engineering Module)

Application mode name: chekf2

5.4.1. Scalar Variables

Name	Variable	Value	Unit	Description
F	F_chekf2	96485.3415	s*A/mol	Faraday's constant

5.4.2. Application Mode Properties

Property	**Value**
Default element type	Lagrange - Quadratic
Analysis type	Transient
Equation form	Non-conservative
Equilibrium assumption	Off
Frame	Frame (ref)
Weak constraints	Off
Constraint type	Ideal

5.4.3. Variables

Dependent variables: cb

Shape functions: shlag(2,'cb')

Interior boundaries not active

5.4.4. Boundary Settings

Boundary		4, 8, 13, 17, 21, 25-28	6, 19	12
Type		Insulation/Symmetry	Flux	Insulation/Symmetry
Inward flux (N)	$mol/(m^2 \cdot s)$	0	**M*(ct-K*cb)**	0
Concentration (c0)	mol/m^3	0	0	**cb0**

5.4.5. Subdomain Settings

Subdomain		2
Diffusion coefficient (D)	m^2/s	**Db**
Mobility (um)	s·mol/kg	**Db/(R*T)**
Charge number (z)	1	**char**
Potential (V)	V	**V**

Isotropic diffusion switch (idon)		**1**
Streamline diffusion switch (sdon)		**1**

Subdomain initial value		2
Concentration, cb (cb)	mol/m^3	cb0

5.5. Application Mode: Conductive Media DC (emdc)

Application mode type: Conductive Media DC (AC/DC Module)

Application mode name: emdc

5.5.1. Scalar Variables

Name	Variable	Value	Unit	Description
epsilon0	epsilon0_emdc	8.854187817e-12	F/m	Permittivity of vacuum
mu0	mu0_emdc	4*pi*1e-7	H/m	Permeability of vacuum

5.5.2. Application Mode Properties

Property	**Value**
Default element type	Lagrange - Quadratic
Input property	Forced voltage
Frame	Frame (ref)
Weak constraints	Off
Constraint type	Ideal

5.5.3. Variables

Dependent variables: V

Shape functions: shlag(2,'V')

Interior boundaries not active

5.5.4. Boundary Settings

Boundary		1-2, 4-5, 8-15, 17-18, 21-28	3	16
Type		Electric insulation	Electric potential	Ground
Electric potential (V0)	V	0	**V0**	**V0**

5.5.5. Subdomain Settings

Subdomain		1-5
Electric conductivity (sigma)	S/m	**{cond,0;0,cond}**

6. Solver Settings

Solve using a script: off

Analysis type	Transient
Auto select solver	On
Solver	Time dependent
Solution form	Automatic
Symmetric	auto
Adaptive mesh refinement	Off
Optimization/Sensitivity	Off
Plot while solving	Off

6.1. Direct (UMFPACK)

Solver type: Linear system solver

Parameter	**Value**
Pivot threshold	0.1
Memory allocation factor	0.7

6.2. Time Stepping

Parameter	**Value**
Times	range(0,5,3600)
Relative tolerance	0.01
Absolute tolerance	0.0010
Times to store in output	Specified times
Time steps taken by solver	Free
Maximum BDF order	5
Singular mass matrix	Maybe
Consistent initialization of DAE systems	Backward Euler
Error estimation strategy	Include algebraic
Allow complex numbers	Off

6.3. Advanced

Parameter	Value
Constraint handling method	Elimination
Null-space function	Automatic
Automatic assembly block size	On
Assembly block size	1000
Use Hermitian transpose of constraint matrix and in symmetry detection	Off
Use complex functions with real input	Off
Stop if error due to undefined operation	On
Store solution on file	Off
Type of scaling	Automatic
Manual scaling	
Row equilibration	On
Manual control of reassembly	Off
Load constant	On
Constraint constant	On
Mass constant	On
Damping (mass) constant	On
Jacobian constant	On
Constraint Jacobian constant	On

7. Postprocessing

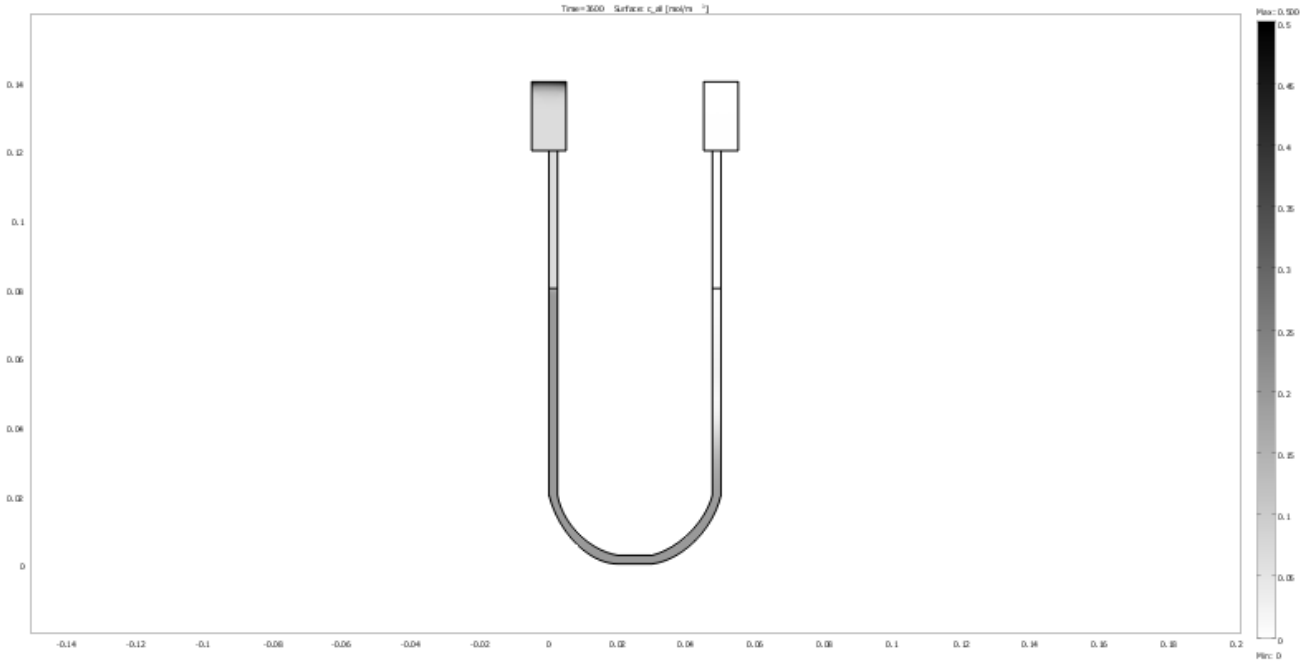

8. Variables

8.1. Boundary

8.1.1. Boundary 1-3, 5, 7, 9-11, 14-16, 18, 20, 22-24

Name	Description	Unit	Expression
ndflux_ct_chekf	Normal diffusive flux, ct	mol/(m^2*s)	nx_chekf * dflux_ct_x_chekf+ny_chekf * dflux_ct_y_chekf
ncflux_ct_chekf	Normal convective flux, ct	mol/(m^2*s)	nx_chekf * cflux_ct_x_chekf+ny_chekf * cflux_ct_y_chekf
nmflux_ct_chekf	Normal electrophoretic flux, ct	mol/(m^2*s)	nx_chekf * mflux_ct_x_chekf+ny_chekf * mflux_ct_y_chekf

ntflux_ct_chekf	Normal total flux, ct	mol/(m^2*s)	nx_chekf * tflux_ct_x_chekf+ny_chekf * tflux_ct_y_chekf
ndflux_cb_chekf2	Normal diffusive flux, cb	mol/(m^2*s)	
ncflux_cb_chekf2	Normal convective flux, cb	mol/(m^2*s)	
nmflux_cb_chekf2	Normal electrophoretic flux, cb	mol/(m^2*s)	
ntflux_cb_chekf2	Normal total flux, cb	mol/(m^2*s)	
dVolbnd_emdc	Volume integration contribution	m	d_emdc
tEx_emdc	Tangential electric field, x component	V/m	-VTx
tEy_emdc	Tangential electric field, y component	V/m	-VTy
normtE_emdc	Tangential electric field, norm	V/m	sqrt(abs(tEx_emdc)^2+abs(tEy_emdc)^2)
nJ_emdc	Normal current density	A/m^2	nx_emdc * Jx_emdc+ny_emdc * Jy_emdc
nJs_emdc	Source current density	A/m^2	unx * (down(Jx_emdc)-up(Jx_emdc))+uny * (down(Jy_emdc)-up(Jy_emdc))
Jsx_emdc	Surface current density, x component	A/m	0
Jsy_emdc	Surface current density, y component	A/m	0
Qs_emdc	Surface resistive heating	W/m^2	Jsx_emdc * tEx_emdc+Jsy_emdc * tEy_emdc
normJs_emdc	Surface current	A/m	sqrt(abs(Jsx_emdc)^2+abs(Jsy_emdc)^2)

	density, norm		

8.1.2. Boundary 4, 8, 12-13, 17, 21, 25-28

Name	Description	Unit	Expression
ndflux_ct_chekf	Normal diffusive flux, ct	mol/(m^2*s)	
ncflux_ct_chekf	Normal convective flux, ct	mol/(m^2*s)	
nmflux_ct_chekf	Normal electrophoretic flux, ct	mol/(m^2*s)	
ntflux_ct_chekf	Normal total flux, ct	mol/(m^2*s)	
ndflux_cb_chekf2	Normal diffusive flux, cb	mol/(m^2*s)	nx_chekf2 * dflux_cb_x_chekf2+ny_chekf2 * dflux_cb_y_chekf2
ncflux_cb_chekf2	Normal convective flux, cb	mol/(m^2*s)	nx_chekf2 * cflux_cb_x_chekf2+ny_chekf2 * cflux_cb_y_chekf2
nmflux_cb_chekf2	Normal electrophoretic flux, cb	mol/(m^2*s)	nx_chekf2 * mflux_cb_x_chekf2+ny_chekf2 * mflux_cb_y_chekf2
ntflux_cb_chekf2	Normal total flux, cb	mol/(m^2*s)	nx_chekf2 * tflux_cb_x_chekf2+ny_chekf2 * tflux_cb_y_chekf2
dVolbnd_emdc	Volume integration contribution	m	d_emdc
tEx_emdc	Tangential electric field, x component	V/m	-VTx
tEy_emdc	Tangential electric field, y component	V/m	-VTy
normtE_emdc	Tangential electric field, norm	V/m	sqrt(abs(tEx_emdc)^2+abs(tEy_emdc)^2)
nJ_emdc	Normal current density	A/m^2	nx_emdc * Jx_emdc+ny_emdc * Jy_emdc
nJs_emdc	Source	A/m^2	unx * (down(Jx_emdc)-

	current density		up(Jx_emdc))+uny * (down(Jy_emdc)-up(Jy_emdc))
Jsx_emdc	Surface current density, x component	A/m	0
Jsy_emdc	Surface current density, y component	A/m	0
Qs_emdc	Surface resistive heating	W/m^2	Jsx_emdc * tEx_emdc+Jsy_emdc * tEy_emdc
normJs_emdc	Surface current density, norm	A/m	sqrt(abs(Jsx_emdc)^2+abs(Jsy_emdc)^2)

8.1.3. Boundary 6, 19

Name	Description	Unit	Expression
ndflux_ct_chekf	Normal diffusive flux, ct	mol/(m^2*s)	nx_chekf * dflux_ct_x_chekf+ny_chekf * dflux_ct_y_chekf
ncflux_ct_chekf	Normal convective flux, ct	mol/(m^2*s)	nx_chekf * cflux_ct_x_chekf+ny_chekf * cflux_ct_y_chekf
nmflux_ct_chekf	Normal electrophoretic flux, ct	mol/(m^2*s)	nx_chekf * mflux_ct_x_chekf+ny_chekf * mflux_ct_y_chekf
ntflux_ct_chekf	Normal total flux, ct	mol/(m^2*s)	nx_chekf * tflux_ct_x_chekf+ny_chekf * tflux_ct_y_chekf
ndflux_cb_chekf2	Normal diffusive flux, cb	mol/(m^2*s)	nx_chekf2 * dflux_cb_x_chekf2+ny_chekf2 * dflux_cb_y_chekf2
ncflux_cb_chekf2	Normal convective flux, cb	mol/(m^2*s)	nx_chekf2 * cflux_cb_x_chekf2+ny_chekf2 * cflux_cb_y_chekf2
nmflux_cb_chekf2	Normal electrophoretic flux, cb	mol/(m^2*s)	nx_chekf2 * mflux_cb_x_chekf2+ny_chekf2 * mflux_cb_y_chekf2
ntflux_cb_chekf2	Normal total flux, cb	mol/(m^2*s)	nx_chekf2 * tflux_cb_x_chekf2+ny_chekf2 * tflux_cb_y_chekf2
dVolbnd_emdc	Volume	m	d_emdc

	integration contribution		
tEx_emdc	Tangential electric field, x component	V/m	-VTx
tEy_emdc	Tangential electric field, y component	V/m	-VTy
normtE_emdc	Tangential electric field, norm	V/m	sqrt(abs(tEx_emdc)^2+abs(tEy_emdc)^2)
nJ_emdc	Normal current density	A/m^2	nx_emdc * Jx_emdc+ny_emdc * Jy_emdc
nJs_emdc	Source current density	A/m^2	unx * (down(Jx_emdc)-up(Jx_emdc))+uny * (down(Jy_emdc)-up(Jy_emdc))
Jsx_emdc	Surface current density, x component	A/m	0
Jsy_emdc	Surface current density, y component	A/m	0
Qs_emdc	Surface resistive heating	W/m^2	Jsx_emdc * tEx_emdc+Jsy_emdc * tEy_emdc
normJs_emdc	Surface current density, norm	A/m	sqrt(abs(Jsx_emdc)^2+abs(Jsy_emdc)^2)

8.2. Subdomain

8.2.1. Subdomain 1, 3-5

Name	Description	Unit	Expression
grad_ct_x_chekf	Concentration gradient, ct, x component	mol/m^4	ctx
dflux_ct_x_chekf	Diffusive flux, ct, x	mol/(m^2*s)	-Dxx_ct_chekf * ctx-Dxy_ct_chekf * cty

	component		
cflux_ct_x_chekf	Convective flux, ct, x component	mol/(m^2*s)	ct * u_ct_chekf
mflux_ct_x_chekf	Electrophoretic flux, ct, x component	mol/(m^2*s)	-z_ct_chekf * um_ct_chekf * F_chekf * ct * gradpot_ct_x_chekf
tflux_ct_x_chekf	Total flux, ct, x component	mol/(m^2*s)	dflux_ct_x_chekf+cflux_ct_x_chekf+mflux_ct_x_chekf
grad_ct_y_chekf	Concentration gradient, ct, y component	mol/m^4	cty
dflux_ct_y_chekf	Diffusive flux, ct, y component	mol/(m^2*s)	-Dyx_ct_chekf * ctx-Dyy_ct_chekf * cty
cflux_ct_y_chekf	Convective flux, ct, y component	mol/(m^2*s)	ct * v_ct_chekf
mflux_ct_y_chekf	Electrophoretic flux, ct, y component	mol/(m^2*s)	-z_ct_chekf * um_ct_chekf * F_chekf * ct * gradpot_ct_y_chekf
tflux_ct_y_chekf	Total flux, ct, y component	mol/(m^2*s)	dflux_ct_y_chekf+cflux_ct_y_chekf+mflux_ct_y_chekf
beta_ct_x_chekf	Convective field, ct, x component	m/s	u_ct_chekf-z_ct_chekf * um_ct_chekf * F_chekf * gradpot_ct_x_chekf
beta_ct_y_chekf	Convective field, ct, y component	m/s	v_ct_chekf-z_ct_chekf * um_ct_chekf * F_chekf * gradpot_ct_y_chekf
grad_ct_chekf	Concentration gradient, ct	mol/m^4	sqrt(grad_ct_x_chekf^2+grad_ct_y_chekf^2)
dflux_ct_chekf	Diffusive flux, ct	mol/(m^2*s)	sqrt(dflux_ct_x_chekf^2+dflux_ct_y_chekf^2)
cflux_ct_chekf	Convective flux, ct	mol/(m^2*s)	sqrt(cflux_ct_x_chekf^2+cflux_ct_y_chekf^2)
mflux_ct_chekf	Electrophoretic flux, ct	mol/(m^2*s)	sqrt(mflux_ct_x_chekf^2+mflux_ct_y_chekf^2)
tflux_ct_chekf	Total flux,	mol/(m^2	sqrt(tflux_ct_x_chekf^2+tflux_ct_y_chekf^2)

	ct	*s)	
cellPe_ct_chekf	Cell Peclet number, ct	1	h * sqrt(beta_ct_x_chekf^2+beta_ct_y_chekf^2)/Dm_ct_chekf
Dm_ct_chekf	Mean diffusion coefficient, ct	m^2/s	(Dxx_ct_chekf * (u_ct_chekf-z_ct_chekf * um_ct_chekf * F_chekf * gradpot_ct_x_chekf)^2+Dxy_ct_chekf * (u_ct_chekf-z_ct_chekf * um_ct_chekf * F_chekf * gradpot_ct_x_chekf) * (v_ct_chekf-z_ct_chekf * um_ct_chekf * F_chekf * gradpot_ct_y_chekf)+Dyx_ct_chekf * (v_ct_chekf-z_ct_chekf * um_ct_chekf * F_chekf * gradpot_ct_y_chekf) * (u_ct_chekf-z_ct_chekf * um_ct_chekf * F_chekf * gradpot_ct_x_chekf)+Dyy_ct_chekf * (v_ct_chekf-z_ct_chekf * um_ct_chekf * F_chekf * gradpot_ct_y_chekf)^2)/((u_ct_chekf-z_ct_chekf * um_ct_chekf * F_chekf * gradpot_ct_x_chekf)^2+(v_ct_chekf-z_ct_chekf * um_ct_chekf * F_chekf * gradpot_ct_y_chekf)^2+eps)
res_ct_chekf	Equation residual for ct	mol/(m^3*s)	-Dxx_ct_chekf * ctxx-Dxy_ct_chekf * ctxy+ctx * (u_ct_chekf-z_ct_chekf * um_ct_chekf * F_chekf * gradpot_ct_x_chekf)-Dyx_ct_chekf * ctyx-Dyy_ct_chekf * ctyy+cty * (v_ct_chekf-z_ct_chekf * um_ct_chekf * F_chekf * gradpot_ct_y_chekf)-R_ct_chekf
res_sc_ct_chekf	Shock capturing residual for ct	mol/(m^3*s)	ctx * (u_ct_chekf-z_ct_chekf * um_ct_chekf * F_chekf * gradpot_ct_x_chekf)+cty * (v_ct_chekf-z_ct_chekf * um_ct_chekf * F_chekf * gradpot_ct_y_chekf)-R_ct_chekf
da_ct_chekf	Total time scale factor, ct	1	Dts_ct_chekf
gradpot_ct_x_chekf	Potential gradient, ct, x component	V/m	d(V,x)
gradpot_ct_y_chekf	Potential gradient, ct, y component	V/m	d(V,y)
grad_cb_x_chekf2	Concentration gradient,	mol/m^4	

	cb, x component		
dflux_cb_x_chekf2	Diffusive flux, cb, x component	mol/(m^2*s)	
cflux_cb_x_chekf2	Convective flux, cb, x component	mol/(m^2*s)	
mflux_cb_x_chekf2	Electrophoretic flux, cb, x component	mol/(m^2*s)	
tflux_cb_x_chekf2	Total flux, cb, x component	mol/(m^2*s)	
grad_cb_y_chekf2	Concentration gradient, cb, y component	mol/m^4	
dflux_cb_y_chekf2	Diffusive flux, cb, y component	mol/(m^2*s)	
cflux_cb_y_chekf2	Convective flux, cb, y component	mol/(m^2*s)	
mflux_cb_y_chekf2	Electrophoretic flux, cb, y component	mol/(m^2*s)	
tflux_cb_y_chekf2	Total flux, cb, y component	mol/(m^2*s)	
beta_cb_x_chekf2	Convective field, cb, x component	m/s	
beta_cb_y_chekf2	Convective field, cb, y component	m/s	
grad_cb_chekf2	Concentration gradient, cb	mol/m^4	
dflux_cb_chekf2	Diffusive flux, cb	mol/(m^2*s)	
cflux_cb_chekf2	Convective	mol/(m^2	

	flux, cb	*s)	
mflux_cb_chekf2	Electrophoretic flux, cb	mol/(m^2*s)	
tflux_cb_chekf2	Total flux, cb	mol/(m^2*s)	
cellPe_cb_chekf2	Cell Peclet number, cb	1	
Dm_cb_chekf2	Mean diffusion coefficient, cb	m^2/s	
res_cb_chekf2	Equation residual for cb	mol/(m^3*s)	
res_sc_cb_chekf2	Shock capturing residual for cb	mol/(m^3*s)	
da_cb_chekf2	Total time scale factor, cb	1	
gradpot_cb_x_chekf2	Potential gradient, cb, x component	V/m	
gradpot_cb_y_chekf2	Potential gradient, cb, y component	V/m	
dr_guess_emdc	Width in radial direction default guess	m	0
R0_guess_emdc	Inner radius default guess	m	0
Sx_emdc	Infinite element x coordinate	m	x
S0x_guess_emdc	Inner x coordinate default guess	m	0

Sdx_guess_emdc	Width in x direction default guess	m	0
Sy_emdc	Infinite element y coordinate	m	y
S0y_guess_emdc	Inner y coordinate default guess	m	0
Sdy_guess_emdc	Width in y direction default guess	m	0
dVol_emdc	Volume integration contribution	m	detJ_emdc * d_emdc
sigma_emdc	Electric conductivity	S/m	sigmaxx_emdc
Jix_emdc	Induced current density, x component	A/m^2	sigmaxx_emdc * Ex_emdc
Jiy_emdc	Induced current density, y component	A/m^2	sigmayy_emdc * Ey_emdc
Ex_emdc	Electric field, x component	V/m	-Vx
Ey_emdc	Electric field, y component	V/m	-Vy
Jx_emdc	Total current density, x component	A/m^2	Jex_emdc+Jix_emdc
Jy_emdc	Total current density, y component	A/m^2	Jey_emdc+Jiy_emdc
Q_emdc	Resistive heating	W/m^3	Jx_emdc * Ex_emdc+Jy_emdc * Ey_emdc

8.2.2. Subdomain 2

Name	Description	Unit	Expression
grad_ct_x_chekf	Concentration gradient, ct, x component	mol/m^4	
dflux_ct_x_chekf	Diffusive flux, ct, x component	mol/(m^2*s)	
cflux_ct_x_chekf	Convective flux, ct, x component	mol/(m^2*s)	
mflux_ct_x_chekf	Electrophoretic flux, ct, x component	mol/(m^2*s)	
tflux_ct_x_chekf	Total flux, ct, x component	mol/(m^2*s)	
grad_ct_y_chekf	Concentration gradient, ct, y component	mol/m^4	
dflux_ct_y_chekf	Diffusive flux, ct, y component	mol/(m^2*s)	
cflux_ct_y_chekf	Convective flux, ct, y component	mol/(m^2*s)	
mflux_ct_y_chekf	Electrophoretic flux, ct, y component	mol/(m^2*s)	
tflux_ct_y_chekf	Total flux, ct, y component	mol/(m^2*s)	
beta_ct_x_chekf	Convective field, ct, x component	m/s	
beta_ct_y_chekf	Convective	m/s	

	field, ct, y component		
grad_ct_chekf	Concentration gradient, ct	mol/m^4	
dflux_ct_chekf	Diffusive flux, ct	mol/(m^2*s)	
cflux_ct_chekf	Convective flux, ct	mol/(m^2*s)	
mflux_ct_chekf	Electrophoretic flux, ct	mol/(m^2*s)	
tflux_ct_chekf	Total flux, ct	mol/(m^2*s)	
cellPe_ct_chekf	Cell Peclet number, ct	1	
Dm_ct_chekf	Mean diffusion coefficient, ct	m^2/s	
res_ct_chekf	Equation residual for ct	mol/(m^3*s)	
res_sc_ct_chekf	Shock capturing residual for ct	mol/(m^3*s)	
da_ct_chekf	Total time scale factor, ct	1	
gradpot_ct_x_chekf	Potential gradient, ct, x component	V/m	
gradpot_ct_y_chekf	Potential gradient, ct, y component	V/m	
grad_cb_x_chekf2	Concentration gradient, cb, x component	mol/m^4	cbx
dflux_cb_x_chekf2	Diffusive flux, cb, x	mol/(m^2*s)	-Dxx_cb_chekf2 * cbx-Dxy_cb_chekf2 * cby

	component		
cflux_cb_x_chekf2	Convective flux, cb, x component	mol/(m^2*s)	cb * u_cb_chekf2
mflux_cb_x_chekf2	Electrophoretic flux, cb, x component	mol/(m^2*s)	-z_cb_chekf2 * um_cb_chekf2 * F_chekf2 * cb * gradpot_cb_x_chekf2
tflux_cb_x_chekf2	Total flux, cb, x component	mol/(m^2*s)	dflux_cb_x_chekf2+cflux_cb_x_chekf2+mflux_cb_x_chekf2
grad_cb_y_chekf2	Concentration gradient, cb, y component	mol/m^4	cby
dflux_cb_y_chekf2	Diffusive flux, cb, y component	mol/(m^2*s)	-Dyx_cb_chekf2 * cbx-Dyy_cb_chekf2 * cby
cflux_cb_y_chekf2	Convective flux, cb, y component	mol/(m^2*s)	cb * v_cb_chekf2
mflux_cb_y_chekf2	Electrophoretic flux, cb, y component	mol/(m^2*s)	-z_cb_chekf2 * um_cb_chekf2 * F_chekf2 * cb * gradpot_cb_y_chekf2
tflux_cb_y_chekf2	Total flux, cb, y component	mol/(m^2*s)	dflux_cb_y_chekf2+cflux_cb_y_chekf2+mflux_cb_y_chekf2
beta_cb_x_chekf2	Convective field, cb, x component	m/s	u_cb_chekf2-z_cb_chekf2 * um_cb_chekf2 * F_chekf2 * gradpot_cb_x_chekf2
beta_cb_y_chekf2	Convective field, cb, y component	m/s	v_cb_chekf2-z_cb_chekf2 * um_cb_chekf2 * F_chekf2 * gradpot_cb_y_chekf2
grad_cb_chekf2	Concentration gradient, cb	mol/m^4	sqrt(grad_cb_x_chekf2^2+grad_cb_y_chekf2^2)
dflux_cb_chekf2	Diffusive flux, cb	mol/(m^2*s)	sqrt(dflux_cb_x_chekf2^2+dflux_cb_y_chekf2^2)
cflux_cb_chekf2	Convective flux, cb	mol/(m^2*s)	sqrt(cflux_cb_x_chekf2^2+cflux_cb_y_chekf2^2)
mflux_cb_chekf	Electropho	mol/(m^	sqrt(mflux_cb_x_chekf2^2+mflux_cb_y_chekf2^

2	retic flux, cb	2*s)	2)
tflux_cb_chekf2	Total flux, cb	mol/(m^2*s)	sqrt(tflux_cb_x_chekf2^2+tflux_cb_y_chekf2^2)
cellPe_cb_chekf2	Cell Peclet number, cb	1	h * sqrt(beta_cb_x_chekf2^2+beta_cb_y_chekf2^2) /Dm_cb_chekf2
Dm_cb_chekf2	Mean diffusion coefficient, cb	m^2/s	(Dxx_cb_chekf2 * (u_cb_chekf2-z_cb_chekf2 * um_cb_chekf2 * F_chekf2 * gradpot_cb_x_chekf2)^2+Dxy_cb_chekf2 * (u_cb_chekf2-z_cb_chekf2 * um_cb_chekf2 * F_chekf2 * gradpot_cb_x_chekf2) * (v_cb_chekf2-z_cb_chekf2 * um_cb_chekf2 * F_chekf2 * gradpot_cb_y_chekf2)+Dyx_cb_chekf2 * (v_cb_chekf2-z_cb_chekf2 * um_cb_chekf2 * F_chekf2 * gradpot_cb_y_chekf2) * (u_cb_chekf2-z_cb_chekf2 * um_cb_chekf2 * F_chekf2 * gradpot_cb_x_chekf2)+Dyy_cb_chekf2 * (v_cb_chekf2-z_cb_chekf2 * um_cb_chekf2 * F_chekf2 * gradpot_cb_y_chekf2)^2)/((u_cb_chekf2-z_cb_chekf2 * um_cb_chekf2 * F_chekf2 * gradpot_cb_x_chekf2)^2+(v_cb_chekf2-z_cb_chekf2 * um_cb_chekf2 * F_chekf2 * gradpot_cb_y_chekf2)^2+eps)
res_cb_chekf2	Equation residual for cb	mol/(m^3*s)	-Dxx_cb_chekf2 * cbxx-Dxy_cb_chekf2 * cbxy+cbx * (u_cb_chekf2-z_cb_chekf2 * um_cb_chekf2 * F_chekf2 * gradpot_cb_x_chekf2)-Dyx_cb_chekf2 * cbyx-Dyy_cb_chekf2 * cbyy+cby * (v_cb_chekf2-z_cb_chekf2 * um_cb_chekf2 * F_chekf2 * gradpot_cb_y_chekf2)-R_cb_chekf2
res_sc_cb_chekf2	Shock capturing residual for cb	mol/(m^3*s)	cbx * (u_cb_chekf2-z_cb_chekf2 * um_cb_chekf2 * F_chekf2 * gradpot_cb_x_chekf2)+cby * (v_cb_chekf2-z_cb_chekf2 * um_cb_chekf2 * F_chekf2 * gradpot_cb_y_chekf2)-R_cb_chekf2
da_cb_chekf2	Total time scale factor, cb	1	Dts_cb_chekf2
gradpot_cb_x_chekf2	Potential gradient, cb, x	V/m	d(V,x)

	component		
gradpot_cb_y_chekf2	Potential gradient, cb, y component	V/m	d(V,y)
dr_guess_emdc	Width in radial direction default guess	m	0
R0_guess_emdc	Inner radius default guess	m	0
Sx_emdc	Infinite element x coordinate	m	x
S0x_guess_emdc	Inner x coordinate default guess	m	0
Sdx_guess_emdc	Width in x direction default guess	m	0
Sy_emdc	Infinite element y coordinate	m	y
S0y_guess_emdc	Inner y coordinate default guess	m	0
Sdy_guess_emdc	Width in y direction default guess	m	0
dVol_emdc	Volume integration contribution	m	detJ_emdc * d_emdc
sigma_emdc	Electric conductivity	S/m	sigmaxx_emdc
Jix_emdc	Induced	A/m^2	sigmaxx_emdc * Ex_emdc

	current density, x component		
Jiy_emdc	Induced current density, y component	A/m^2	sigmayy_emdc * Ey_emdc
Ex_emdc	Electric field, x component	V/m	-Vx
Ey_emdc	Electric field, y component	V/m	-Vy
Jx_emdc	Total current density, x component	A/m^2	Jex_emdc+Jix_emdc
Jy_emdc	Total current density, y component	A/m^2	Jey_emdc+Jiy_emdc
Q_emdc	Resistive heating	W/m^3	Jx_emdc * Ex_emdc+Jy_emdc * Ey_emdc